January 2008

Vegetation over hydrologic control of sediment transport over the past 100,000 yr

Anthony Dosseto
University of Wollongong, tonyd@uow.edu.au

Simon Turner

P P Hesse

Kate Maher

Kirstie Fryirs
Macquarie University

Vegetation over hydrologic control of sediment transport over the past 100,000 yr

Concentric slow cooling of a low *P*-high *T* terrain: Evidence from 1600-1300 Ma mica dates in the 1780-1700 Ma Black Hills Orogen, South Dakota, USA

P.S. DAHL[1]* AND K.A. FOLAND[2]

[1]Department of Geology, Kent State University, Kent, Ohio 44242 USA (*correspondence: pdahl@kent.edu)
[2]Department of Geological Sciences, Ohio State University, Columbus, Ohio 43210 USA

The crystalline core of the southern Black Hills (SBH), South Dakota, exposes an extensive, low *P*-high *T* aureole of garnet- to 2nd-sillimanite-zone schists centered on the plutonic core of the 1715 Ma Harney Peak Granite (HPG). This paper demonstrates regional patterns of apparent age observed for 52 $^{40}Ar/^{39}Ar$ dates of muscovite and biotite in diverse rocks from across the ~1000-km^2 metamorphic aureole and its plutonic center. About 20 biotite dates, sampled mostly near faults, are influenced by excess ^{40}Ar and obscure the regional trends. The remaining dates reveal radial patterns of apparent younging from outer aureole toward inner granite, with previously unrecognized, elliptical age zones centered on the main HPG pluton and its outliers. The regional pattern of $^{40}Ar/^{39}Ar$ cooling ages indicates non-uniform slow cooling of the mid-crust between ~1600-1250 Ma. This scenario of delayed slow cooling from aureole to pluton is consistent with published cooling ages for muscovite (Rb/Sr) and apatite (U/Pb), which range from 1690 to 1550 Ma and from 1700 to ~1500 Ma, respectively. To explain these results, it is likely that ambient pre-granite temperatures of the country rocks were $\geq$350 °C at the ~10-14 km depth of granite emplacement, as previously proposed, and that the entire complex resided at this depth and cooled slowly from aureole to granite for 100's of m.y. Alternatively, or in addition, the HPG and inner aureole were not uplifted until ~1480-1330 Ma, whereupon they finally cooled through ~350-300 °C.

An age compilation representing diverse SBH minerals reveals a composite sequence of relative isotopic closure comparable to that commonly observed elsewhere: monazite (Pb) > apatite (Hf) > hornblende (Ar) = apatite (Pb) = low-Rb muscovite (Sr) > muscovite (Ar) > biotite (Ar) = apatite (Sr). Likewise, for a given mineral, the retentivity sequence is consistent with ionic radii and/or experiment (cf. Hf, Pb, and Sr in apatite; Sr and Ar in muscovite, etc). This systematic behavior underscores the crystal-chemical basis for isotopic closure phenomena, as formalized elsewhere.

Molybdenum isotope variations in a redox-stratified lake; Removal mechanism and preservation in euxinic sediments

T.W. DAHL[1], A.D. ANBAR[2], G.W. GORDON[2], M.T.ROSING[1], R.E. FREI[1] AND D.E. CANFIELD[1]

[1]NordCEE and Geological Museum, Univ. of Copenhagen, Øster Voldgade 5-7, 1350 Copenhagen K, Denmark
[2]School of Earth & Space Expl. and Dept. of Chem. & Biochem. Ariz. State Univ., Tempe, AZ 85287, USA

The chemical behavior of Molybdenum (Mo) is investigated in a sulfidic lake system to understand the potential of using Mo isotopes as a paleo-redox proxy in euxinic sediments.

Meromictic Lake Cadagno in Switzerland displays a redox gradient with sulfidic bottom waters, which acts as a perfect trap for Mo. Concentrations are elevated by more than 2 orders of magnitude (130ppm) relative to rocks in the catchment area. Isotopically, Mo in the sulfidic water column ($\delta^{98/95}Mo$ = 1.8±0.1‰) is about 1‰ heavier than the riverine source where it adsorbs to >0.2um particles.

The isotope systematics is complicated by a subaquatic source appearing from dolomitic bedrock. A simple model suggests Mo isotope fractionation at the chemocline is associated with conversion of molybdate to particle reactive thiomolybdate, hence the residence time for Mo in the sulfidic zone is comparable to the slow kinetics of these reactions [2]. The isotopic composition in the sediment is constant and we conclude that Mo isotopes are preserved in sulfidic settings through early diagenesis.

[1] Tossel J. A. (2005) *GCA* **69**, 2981-2993. [2] Ericksson & Helz (2000) *GCA* **64**, 1149-1158.

Variable H and O isotopes in Tongan basaltic glasses: Source or degassing?

C.W. DALE[1], C.G. MACPHERSON[1], A.J. BOYCE[2], G.M. NOWELL[1], D.G. PEARSON[1] AND R.J. ARCULUS[3]

[1]Dept of Earth Sciences, Durham University, Durham, DH1 3LE, UK

[2]Scottish Universities Environment Research Centre, East Kilbride, G75 0QF, UK

[3]Dept of Earth & Marine Sciences, Australian National University, ACT 0200, Australia

New H and O isotope data are presented for submarine basaltic and basaltic-andesite glasses dredged from the Tongan arc (north of Tongatapu), the Fonualei Rifts (FR, a nascent backarc spreading centre) and the Mangatolu Triple Junction (MTJ). These data complement a comprehensive trace element and Nd-Sr-Pb-Hf isotope dataset.

The highest δD values (-50‰ to -30‰) occur in the MTJ and FR. There is a positive co-variation between δD and H_2O abundance, initially suggesting addition of a δD-rich H_2O component derived from the subducted slab to the upper mantle source. In this scenario, the most negative values (≥-85‰), which have lower water contents, would represent uncontaminated mantle wedge. This is consistent with a MORB source component (typically -80‰ ± 10‰). However, H_2O concentration and δD also increase with depth of eruption, suggesting that degassing may explain the fractionation observed. In this scenario the highest δD (-40‰ to -30‰) may be typical of the whole arc-backarc mantle source, while the lower values are produced by degassing (whereby D is preferentially incorporated into H_2O rather than melt). Extrapolation to infinite water for the whole arc-FR dataset gives a δD value of ca. -26‰. Samples from the MTJ (n=2) are offset to more elevated δD at similar H_2O contents.

Ba/La ratios are highest at the central Tongan volcanoes, indicating that these have the greatest fluid-mobile trace element flux, but they do not possess complementary high δD. Thus, either the D-rich signature is masked by fractionation during degassing or the trace element flux is partially decoupled from the water flux.

$\delta^{18}O$ values range from 4.6‰ to 6.2‰. There is a poor negative co-variation of $\delta^{18}O$ and δD but this is most likely masked by the effects of H fractionation during degassing. Such a co-variation requires the transfer of an ^{18}O-depleted and D-rich fluid from high-T altered oceanic crust, rather than low-T altered crust or sediment.

Trace element analysis and petrology of Martian meteorite RBT04262

H.A. DALTON[1]*, C.-T.A. LEE[1], A.H. PESLIER[2,3], A.D. BRANDON[2] AND T. LAPEN[4]

[1]Rice Univ., Dept of Earth Science, MS 126, PO Box 1892, Houston, TX 77251, USA (*correspondence: heather.a.dalton@rice.edu) (ctlee@rice.edu)

[2]ARES, NASA JSC, Houston, TX 77058, USA (anne.h.peslier@nasa.gov, alan.d.brandon@nasa.gov)

[3]Jacobs Tech., E.S.C.G., Houston, TX 77058, USA

[4]Univ. of Houston, Dept of Geosciences, Houston, TX 77204, USA (tjlapen@uh.edu)

Major and trace element analysis and element mapping of the newly discovered Martian meteorite RBT04262 reveal two main lithologies: a coarse pyroxene zone (lithology 1), and a finer-grained zone containing pyroxenes and olivine interspersed with shocked plagioclase maskelynite (lithology 2), with a reaction zone between them consisting mainly of Ca-rich pyroxene (lithology 3) [1]. Lithology 1 appears to be a basaltic (melt) cumulate, containing large phenocrystic Fo_{66} olivines within En_{65} pigeonites, as well as aggregates of these materials. Lithology 1 may represent a xenocryst set within lithology 2, composed primarily of maskelynite, Fo_{57} olivine, and high- and low-Ca pyroxenes with minor Ca-phosphates, ilmenite, chromite, and Fe-sulfides, which we interpret to represent the host basaltic magma.

Lithology 1 appears to represent earlier crystallized products based on their more primitive trace-element compositions obtained by LA-ICP-MS. Low-Ca pyroxenes in lithology 1 are depleted in REEs and strongly LREE depleted, whereas low-Ca pyroxenes of lithology 2 have slightly higher REE contents, and only slight depletions in LREE. The reaction zone (lithology 3) has a similar trace element composition to lithology 2 low-Ca pyroxenes. RBT04262 may represent a basaltic magma that has entrained earlier cumulate phases. Although the bulk rock composition has not been reconstructed yet, we find that all mineral phases containing significant amounts of REEs are LREE-depleted to flat (Ca-phosphates) when normalized to C1 chondrites. The lack of significant negative Eu anomalies in the pyroxenes, however, suggests relatively high oxygen fugacities, possibly not too different from what is seen on Earth.

[1] Dalton H. A. *et al.* (2008) *LPSC* **XXXIX**, Abs #2308.

A Hafnium isotopic perspective on the provenance and tectonic setting of allochthonous Neoproterozoic sedimentary sequences in the North Atlantic region

J.S. DALY[1]*, C.L. KIRKLAND[2], R. LAM[3] AND P. SYLVESTER[3]

[1]UCD School of Geological Sciences, University College Dublin, Belfield, Dublin 4, Ireland (*correspondence: stephen.daly@ucd.ie)
[2]Swedish Museum of Natural History, Stockholm, Sweden (kris.kirkland@gmail.com)
[3]Memorial University, Newfoundland, Canada (rlam@mun.ca, pauls@esd.mun.ca)

Alternative reconstructions of the Rodinia Supercontinent have given rise to diverse views on the tectonic setting of various Neoproterozoic sedimentary sequences in the North Atlantic region. These include the late Neoproterozoic Sørøy Succession of Arctic Norway and the Moine Supergroup of Scotland. Reconstructions that place Baltica adjacent to Greenland in the late Neoproterozoic imply an intracratonic setting for these basins (e.g. [1]) and appeal to the far field effects of accretion on the Rodinia margin to explain tectonic events such as the c. 850-820 Ma Porsanger and Knoydartian orogenies. An alternative reconstruction locates the Moine and Sørøy basins on the active periphery of Rodinia facing the Panthallassan Ocean [2]. This continental margin setting permits a more conventional setting for the Porsanger and Knoydartian orogenies. Hf isotopic analysis of dated detrital zircons provides a potential discriminant on the basis that a contribution from juvenile sources is more likely on an active continental margin as opposed to an intracratonic milieu.

[1] Cawood, P.A., Nemchin, A.A., Strachan, R., Prave, T. and Krabbendam, M. (2007) *Journal of the Geological Society, London* **164,** 257-275. [2] Kirkland, C.L., Daly, J.S. and Whitehouse, M.J. (2008) Precambrian Research **160,** 245-276.

Fluorine and Barium remobilization in 2.4 Ga low grade metamorphic carbonate rocks associated with dolomitic banded iron formations in Quadrilátero Ferrífero, Brazil

C. DA MOTA CARVALHO[1], C.A. ROSIÈRE[2] AND B. ORBERGER[1]

[1]Université Paris-Sud 11, UMR IDES 8148 - 91405 Orsay/France (damotacarvalho@gmail.com)
[2]Universidade Federal de Minas Gerais - 31270901 Belo Horizonte/Brazil

The Paleoproterozoic Itabira Group (2,419+/- 19 Ga; Pb-Pb isochron data) is one of the few known sequences in the world hosting dolomitic banded iron formations, in the Quadrilátero Ferrífero mining district. It is located in the south of the São Francisco Craton, a geotectonic unit of Brasiliano age (0.8 – 0.6 Ga). At the base, the BIFs grade vertically and horizontally into platform carbonates. They have preserved primary structures comprising stylolitic Fe-oxides rich micrometric laminae, and millimetric iron oxides concretions. These laminae host also dolomite, Mg-silicates, quartz, minor barite, apatite and fluorite. These minerals also occur as inclusions in the concretions. Dolomite inclusions have rombohedral shapes, different from those in the laminae that show irregular grains with lobate boundaries, due to corrosion by calcite. Similarly, the irregular shapes of Mg-silicates also indicate reactions processes. The Fe-oxide bearing laminae alternate with centimetric bands composed of low-Mg calcite, with traces of Fe, Mn, Ba (<3,500 ppm) and F (<1,000 ppm). They are finely intergrown with Mg-Al-phyllosilicates and quartz. Oblique veins of carbonates and/or fluorite represent probably diagenetically remobilized material. The overall mineralogical assemblage indicates low grade metamorphism in a carbonaceous-siliceous rock transforming a dolostone into a quasi-limestone leading to *in situ* remobilisation/ resequestration of F and Ba.

Mushroom garnet from the Mt. Mucrone, Italian Alps

B. DARBELLAY[1], M. ROBYR[2] AND L. BAUMGARTNER[1]

[1]Institute of Mineralogy and Geochemistry, University of Lausanne, L'Anthropole, 1015 Lausanne, Switzerland
[2]The University of Texas at Austin, Geol Science Dept., 1 University Station C1100, Austin, TX 78712-0254, USA

Garnets have a cubic symmetry, a simple shape and prograde zoning is preserved in low to medium grade rocks. This makes garnets an excellent object for determining PT-t paths and for studying crystal growth mechanisms. But not all zoning patterns are readily understood. Below we present some fascinating and intriguing garnet textures from the Alpine high pressure Mt. Mucrone area (Sesia, Italian Alps).

Pelitic eclogites preserve relic pre-alpine amphibolite to granulite facies mineral assemblages and associated structures. They were overprinted by the alpine high-pressure event(s). Quartz rich layers contain also omphacite, garnet and phengite. High-resolution X-ray tomography images reveal that many garnets are mushroom-shaped in 3D. The garnet core is roundish and poorly connected to the "hat" of the mushroom by a skeletal garnet network grown along quartz-quartz boundaries. The rim totally encloses the core in some cases resulting in a perfect dodecahedral garnet morphology. All intermediate stages between a hat and an atoll garnet structure can be observed.

Garnets are strongly zoned (gros. 19-33%, spes. 0.2-1%, alm. 54-61%, pyr. 7-19%). Three domains can be distinguished: 1) a roundish core at the centre with multiple islands of high Mn concentrations, 2) a middle zone with an extremely complex zoning which is principally composed of an alternation of thin Mg and Fe-rich bands, radiating outwards, perpendicular to the garnet faces, 3) a homogeneous Mn-rich rim. The latter has compositions corresponding to the islands cores located inside the garnet. No miss-orientation between individual zones was detected by EBSD analysis.

These observations suggest: a) multiple garnet generations, with the center being the oldest, which stands in contrast to previous works which suggested dissolution and re-precipitation of the centre; b) garnet rims grew outward and faces also grow sideways; c) garnet growth might have continued inside the rim, even once it crystallized, replacing progressively quartz by widening the initially skeletal network (which followed grain boundaries) and by filling in fractures.

Crystallinity and grain contact mechanics - Neutron TOF scattering in sandstones

T.W. DARLING[1], J.A. TENCATE[2], TH. PROFFEN[3] AND S. VOGEL[3]

[1]Physics Dept., UNR, Reno NV 89557 (darling@unr.edu)
[2]EES-11, LANL, Los Alamos NM 87545 (tencate@lanl.gov)
[3]LANSCE-12, Lujan Center, LANL Los Alamos NM 87545

Previous results on the microscopic distribution of strain in sandstones, as measured by neutron Bragg scattering, compared to the macroscopic sample strain [1] show excess and nonlinear macroscopic strain. We attribute this to deformation of the highly stressed contact regions, not visible to neutron Bragg scattering either due to the smallness of the volume concerned or to a lack of long-range order at the contacts. PDF measurements on the NPDF beamline at LANSCE's Lujan Center have indicated the presence of non long-range ordered silica in sandstones [2], a measurement not in general supported by thin section petrology examination or XRD [3]. We have attempted to verify this result by comparison with neutron signals from nominally completely crystalline, non-bonded assemblages of various sized quartz grains. We present this data which generally supports the existence of non-crystalline silica. The presence of this material at the grain contact may also influence the mechanics of the sample, particularly in the creep, hysteresis, elastic after effects and high frequency nonlinear behaviour, since it occupies a region of high stress around the small grain contact area. We have used the high flux and count rates available at the HIPPO [4] beamline to make (relatively) fast measurements on the response of sandstone samples to temperature changes, while simultaneously measuring the macroscopic elastic properties by a rod-resonance technique. We present this data and discuss the possible influence of non-crystalline contact cementation on the mechanical response of sandstones.

[1] Darling *et al*. (2004) *GRL* **31**, L16604. [2] Page *et al*. (2004) *GRL* **31**, L24606. [3] Private comm. R. Warren / S. Chipera. [4] Vogel *et al*. (2004) *Powder Diff.* **19**, 64-68.

A combined "top down" and "bottom's up" approach to crystal records: Chemical and textural quantification of crystal populations at Mount Hood, Oregon

C. DARR AND A.J.R. KENT*

Oregon State University, Corvallis, OR, 97330, USA
(*correspondence: adam.kent@geo.oregonstate.edu)

Crystal populations carry important information regarding the nature and evolution of mgamatic systems. We present results from Mount Hood, Oregon, where we combine quantitative characterization of crystal populations using crystal size distributions (CSD) with *in situ* trace element analysis of individual crystalline phases. This powerful approach allows us to use CSD to recognize populations of crystals with common histories, and to use trace element compositions to examine the origin of individual populations.

Mount Hood consists primarily of andesitic lavas and associated rocks, and the current edifice has grown over the last ~500 ka. Eruptive products are remarkably homogeneous, >80% of lavas have SiO_2 between 57-63 wt.%, although textural and chemical trends suggest extensive magma mixing and mineral-melt disequilibrium throughout the lifetime of the volcano.

CSD of plagioclase are remarkably consistent. Five out the six lavas studied, ranging in age from 475 ka to 200 years, show concave up CSD, with two distinct line segments characteristic of two distinct crystal populations. We interpret this to reflect mixing of two magmas and this is supported by trace element analyses. Plagioclase from the smaller plagioclase population are enriched in Sr and Ti and depleted in Ba and REE for a given anorthite content, consistent with crystallization from relatively mafic magma. The larger population have lower Sr and Ti and crystallized from more evolved magmas. Crystal residence times are several decades for the larger felsic-derived population and <10 years for smaller crystals. Moreover narrow rims (< 50 μm) on larger crystals have trace elements compositions that match the smaller mafic crystal population. Thus we suggest that mixing occurred late and probably immediately prior to eruption. Overall Mount Hood has been characterized by repeated episodes of mixing between felsic and mafic magmas followed rapidly by eruption. The near constancy of this mixing over ~475 ka implies long term steady state behavior of the magma supply system

Incorporation of Te and Se into ferromanganese (oxyhydr)oxides: The XAFS evidence

A. DAS* AND Y. TAKAHASHI

Hiroshima University, Higashi-Hiroshima, Hiroshima-739 8526, Japan
(*correspondence: anirban-das@hiroshima-u.ac.jp)

Introduction

Tellurium is found enriched (relative to the continental crust) in marine ferromanganese (oxyhydr)oxides (FMO) by factors of ~5000-50000, much higher than any other element including its chemical homologue, Se. We have attempted to investige the mechanism(s) of Te incorporation and its enrichment in FMOs by probing in atomic enviroment using X-ray Absorption Fine Structure (XAFS) spectroscopy and compare the result to that of Se. We report the preliminary findings of the XAFS studies done on a FMO sample and laboratory adsorption experiments of Te and Se on Fe and Mn-oxides.

Results and Discussions

Tellurium K-edge XAFS measurements were carried out at the beamline BL01B1 at SPring-8 (Hyogo, Japan) and Se measurements were made at Photon Factory KEK (Tsukuba, Japan). Data analysis was done using the software REX2000 (Rigaku Co. Ltd.) following standard procedures.

The Te-XANES spectra of AD-14 show that it is roughly similar to that of $Na_2H_4TeO_6$ (w.r.t position of absorption edge energy and shape of spectrum), indicating that Te exists in +VI state in the FMO. This suggests that Te is incorporated into FMO from seawater as +VI and/or oxidized (on Fe (Mn) oxides) to +VI from +IV, after its incorporation. Both (+IV and +VI) states exist in seawater. Lower abundance of Se in FMO restricts the Se-XANES measurement.

The EXAFS spectra of samples reveal that Te and Se are linked to O in their first shell and Fe on their second shell. This probably suggests that under oxic marine conditions oxyanions of Te and Se are adsorbed onto the surfaces of FMOs and are associated with Fe-oxide phase. Eh-pH diagrams, pK values of their oxyanions, in conjunction with the preliminary XAFS data show that Te is enriched in FMOs because of the formation of strong inner-sphere complexation of Te at both +IV and +VI states with Fe as compared to the thermodynamically stable and dominant species of Se in seawater, Se(+VI), which prefers outer-sphere complexes.

We need to investigate in more details by performing laboratory experiments on adsorption of Se and Te on Fe- and Mn-oxides and, careful analyses of more natural FMO samples to corroborate our preliminary findings.

Fractionated mercury isotope in sediments: A quest for processes

RESHMI DAS[12] AND LEROY ODOM[12]

[1]Department of Geological Sciences, Florida State University, Tallahassee, FL, 32306

[2]National High Magnetic Field Laboratory, Tallahassee, Fl, 32310 (das@magnet.fsu.edu)

Analyses of mercury isotopes in sediments from lakes and oceans have revealed mass independent fractionation (MIF) effects. MIF of Hg isotopes can provide constraints on models of Hg cycling in aquatic systems. Isotope ratios $^{198}Hg/^{202}Hg$, $^{199}Hg/^{202}Hg$, $^{200}Hg/^{202}Hg$, $^{201}Hg/^{202}Hg$ and $^{204}Hg/^{202}Hg$ have been measured in mercury vapor generated by reduction of sample solutions with $SnCl_2$ in a continuous- flow cold-vapor generator connected to a Thermo-Finnigan Neptune MC-ICPMS, using a standard-sample bracketing technique, relative to the NIST SRM 3133 Hg-standard. When corrected for mass dependent fractionation, only values for $^{199}Hg/^{202}Hg$ and $^{201}Hg/^{202}Hg$ yield non-zero residuals. These residuals are expressed as $\Delta^{199}Hg$ and $\Delta^{201}Hg$ respectively and have negative or positive values indicating depletion or enrichment.

Lake Erie and Yucatan limestone are enriched in the odd A isotopes. The absolute value of enrichment/depletion generally increases with the depth of the sediment but is not correlated with the total concentration of Hg in the sediments. The primary species of Hg in sediments are Hg(II) and MeHg. The former is scavenged from the water column because of its high reactivity with particulates and MeHg is produced in the anaerobic sediments by sulfate reducing bacteria. Lab experiments have shown that photo-reduction of Hg(II) and MeHg in water yields residual water enriched in the odd_A isotopes (positive $\Delta^{199}Hg$ and $\Delta^{201}Hg$) and liberates elemental Hg that should be depleted in $\Delta^{199}Hg$ and $\Delta^{201}Hg$. Lake Erie and Yucatan sediments might have a large proportion of Hg derived from the water column that retain the odd A isotope enrichment signature. Lake and spring sediments were highly enriched in organics and exhibit negative values of $\Delta^{199}Hg$ and $\Delta^{201}Hg$. The slight depletion of the odd N isotopes in these sediments might be due to the organics, mostly plant materials that derive their ^{199}Hg and ^{201}Hg depletion from the atmosphere and they overwhelm the proportion of enriched ^{199}Hg and ^{201}Hg signature that comes from the adsorped Hg(II) in water. From the range of values of the $\Delta^{201}Hg/\Delta^{199}Hg$ ratios, we infer multiple isotope effects responsible for the MIF.

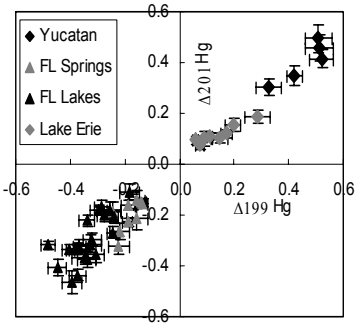

Figure 1: MIF of Hg in sediments.

High-pressure melting relations in Fe-C-S systems: Implications for metallic cores in planetary bodies

R. DASGUPTA[1,2]*, G. WHELAN[1], A. BUONO[1] AND D. WALKER[1]

[1]Lamont-Doherty Earth Observatory, Columbia University, 61 Route 9W, Palisades, NY 10964, USA

[2]Dept of Earth Science, Rice University, Houston, TX 77005, USA (*correspondence: Rajdeep.Dasgupta@rice.edu)

The density deficit of the Earth's outer core with respect to that of pure metallic Fe-liquid suggests presence of ~10% light elements in Earth's outer core. The presence of minor elements such as S, C, O, H, Si, and P is also argued for cores of other planetary bodies. However, experimental data on the effect of light elements on melting relations of Fe in multi-component systems and the mutual solubility of various light elements in molten Fe has been limited.

We investigated the near-liquidus phase relations in Fe-C-S ternary at 2-6 GPa and 1050-1700 °C. Experiments were performed in a piston cylinder and a multi-anvil device using MgO (Fe-5wt.%C-5wt.%S and Fe-5wt.%C-15wt.%S) and graphite (Fe-13%S, Fe-5%S, Fe-1.4%S) capsules. Run products were analyzed for Fe, S, C, and O using electron microprobe.

Liquidus temperature increases from ~1125 °C to ~1410 °C and from ~1100 °C to ~1300 °C from 2 to 6 GPa for Fe-5wt.%C-5wt.%S and Fe-5wt.%C-15wt.%S respectively. The crystalline phase at the liquidus is Fe_3C at 2-4 GPa and Fe_7C_3 at 6 GPa and pure Fe starts crystallizing only with further drop in temperature of ~75 (at 2 GPa) to 200 °C (at 6 GPa) below the liquidus. The melt in equilibrium with crystalline Fe-carbide is S-rich with C/(C+S) weight ratio as low as 0.01 at low-T and high extent of crystallization. For Fe-5wt.%C-5wt.%S, a single liquid is observed above the liquidus at all pressures. But for Fe-5wt.%C-15wt.%S, super-liquidus conditions produce two immiscible liquids at 2-4 GPa and a single liquid at 6 GPa. Liquid immiscibility in Fe-C-S system with high S content can be reconciled with our graphite saturated experiments that show a decrease in C solubility in molten metallic liquid with increasing S content.

Our results along with the 1 atm phase relations in Fe-C-S systems indicate that the mutual solubility of C and S in molten Fe is enhanced with pressure and no liquid immiscibility induced compositional stratification is expected for planetary cores with pressures $\geq$ 6 GPa. But for planetary bodies with core pressures < 6 GPa, a compositional stratification with sulfide-rich outer core and Fe_3C-Fe bearing inner core can be produced.

^{60}Fe in the cosmic blender

N. DAUPHAS[1], D.L. COOK[2], A. SACARABANY[1], C. FRÖHLICH[3], A.M. DAVIS[1], M. WADHWA[4], A. POURMAND[1], T.RAUSCHER[5] AND R. GALLINO[6]

[1]Origins Laboratory, Department of the Geophysical Sciences and Enrico Fermi Institute, The University of Chicago (dauphas@uchicago.edu)
[2]Department of Chemistry and Chemical Biology, Rutgers University
[3]Department of Astronomy and Astrophysics, Enrico Fermi Institute, The University of Chicago
[4]School of Earth and Space Exploration, Arizona State University
[5]Departement für Physik, Universität Basel
[6]Dipartimento di Fisica Generale dell'Universita' di Torino

Central to the significance of ^{60}Fe ($t_{1/2}$=1.49 Myr) in cosmochemistry are the questions of its abundance and distribution in the protoplanetary disk [1-5]. Significant advances have been made recently in estimating the initial ^{60}Fe/^{56}Fe ratio in meteoritic materials [4-7]. The best estimate of the ^{60}Fe/^{56}Fe ratio at the time of CAI formation is 5 to 10×10^{-7}. Several studies have suggested that ^{60}Fe was heterogeneously distributed in the disk [8-10]. In order to address the question of ^{60}Fe distribution, we have analyzed the Ni and Fe isotopic compositions of meteorites already analyzed for Ni by [11]. After internal normalization to constant ^{62}Ni/^{58}Ni and ^{57}Fe/^{54}Fe ratios, meteoritic metal has terrestrial isotopic composition [12]. This result agrees with previous studies but with significantly improved precision [11, 13-15]. We report the most precise measurements of the low abundance neutron-rich isotopes ^{58}Fe and ^{64}Ni (±0.3 ε and ±0.1 ε, respectively). These isotopes are produced together with ^{60}Fe in cc-SN and AGB stars by neutron-capture reactions. Based on the lack of anomalies on ε^{58}Fe, ε^{60}Ni, and ε^{64}Ni and on comparison with model predictions for collateral isotope effects, we conclude that ^{60}Fe must have been injected into the protosolar nebula and mixed to less than 10 % heterogeneity before formation of planetary bodies.

[1] Birck & Lugmair (1988) *EPSL* **90**, 131. [2] Shukolyukov and Lugmair (1993) *Science* **259**, 1138. [3] Wasserburg *et al*. (1998) *ApJ* **500**, L189. [4] Mostefaoui *et al*. (2005) *ApJ* **625**, 271. [5] Tachibana *et al*. (2006) *ApJ* **639**, L87. [6] Tachibana & Huss (2003) *ApJ* **588**, L41. [7] Guan *et al*. (2007) *GCA* **71**, 4082. [8] Sugiura *et al*. (2006) *Earth Planets Space* **58**, 1079. [9] Bizzarro *et al*. (2007) *Science* **316**, 1178. [10] Quitté *et al*. (2007) *LPSC* **38**, #1900. [11] Cook *et al*. (2006) *Anal. Chem.* **78**, 8477. [12] Dauphas *et al*. (2007) *ApJ*, submitted. [13] Quitté *et al*. (2006) *EPSL* **242**, 16. [14] Chen *et al*. (2007) *LPSC* **38**, #1753. [15] Dauphas *et al*. (2004) *Anal. Chem.* **76**, 5855.

Combining experimental studies and kinetic modelling to investigate the carbonation of Ca-bearing silicates

D. DAVAL[1,2]*, I. MARTINEZ[1], J. CORVISIER[2], N. FINDLING[2], B. GOFFE[2] AND F. GUYOT[1,3]

[1]IPGP, Paris, France (*correspondence: daval@ipgp.jussieu.fr)
[2]Laboratoire de Géologie, ENS, CNRS, Paris, France
[3]IMPMC, Paris, France (guyot@lmcp.jussieu.fr)

Among the different ways considered to store CO_2, the safest one involves its conversion into a geologically stable form: carbonate. If the corresponding carbonation proces is thermodynamically favoured for (ultra)basic minerals, only a few data are available for its kinetics. As wollastonite carbonation is thought to be a relevant model to study the kinetics and mechanisms involved during the carbonation process, it was investigated in batch reactors, at realistics pressure and temperature conditions of injection.

The micro-textural features of the neo-formed phases are found to be dependent on the reactions conditions. A silica layer always surrounds the remaining wollastonite grains. Calcites form either packed and continuous coatings of small crystals on (and even interlayered with) this layer if the reaction takes place in supercritical CO_2 or in aqueous fluid with circum-neutral pH, or big and isolated crystals in more acidic fluid. The experimental carbonation rate in the aqueous phase, which is faster than in supercritical CO_2, was compared with kinetic modelling performed with a geochemical code. At acidic pH, comparison of the experimental data with the model shows that the rate-limiting step of the reaction is wollastonite dissolution, and that the passivating effect of the silica layer remains weak. At circum-neutral pH, the experimental data are consistent with an inhibitor effect of the dense calcite coating, which reduces the reactive surface of the wollastonite.

Finally, because the dissolution step is rate-limiting of the carbonation of Ca-bearing silicates, the accuracy of the kinetic modelling strongly depends on the features of the dissolution kinetic rate law implemented in the code. We thus cast doubt on the relevance of the use of classical codes in which reaction rates and chemical affinity are linked by the transition state theory (TST). We have developed an alternative kinetic module which allows the test of more recent mathematical relations than that established using the TST. This shows that the use of TST can be the source of dramatic overestimations of carbonation rates.

Water storage and amphibole control in arc magma differentiation

J.P. DAVIDSON[1], S.P. TURNER[2] AND C.G. MACPHERSON[1]

[1]Dept. of Earth Sciences, University of Durham, Durham DH1 3LE, UK (j.p.davidson@durham.ac.uk, colin.macpherson@durham.ac.uk)

[2]GEMOC, Dept. of Earth & Planetary Sciences, Macquarie University, NSW 2109, Australia (sturner@els.mq.edu.au)

Arc magmas are distinguished from those of other tectonic settings by several first order characteristics; 1) they tend to be realtively differentiated with even the most mafic rocks in a suite typically $\geq 50\%$ SiO_2, 2) they typically contain high H_2O contents and 3) they have distinctive trace element signatures. The "standard" model for arc petrogenesis involves melting of a mantle wedge, preconditioned by the ingress of fluids ± melts from the subducted slab (oceanic crust ± sediments). This produces primitive hydrous basalts with a distinct trace element signature reflecting a combination of process and inheritance from source components. The subsequent differentiation path is critical in defining the compositions of rocks ultimately formed through eruption or emplacement, and also for dictating practical criteria such as eruptive behavior. A petrographic survey of volcanic arc rocks show that they are typically in equilibrium with a shallow pressure gabbroic assemblage. On the other hand, indications of open system processes along with thermal modeling argue for processing in the deep crust.

We have collated data from single volcanic suites from a representative global sample of arcs, and found compelling evidence for the involvement of amphibole during differentiation. Preferential sequestration of middle REE (e.g. Dy) over heavy and light REE can only reasonably be explained by the involvement of amphibole, which has middle REE partition coefficients higher than both light and heavy. Amphibole also, by virtue of its low SiO_2, has the capacity to leverage liquid SiO_2 towards higher values, and may also lower TiO_2 as seen in arc magmas. The amphibole could be directly fractionated from liquids in which it is stable, or residual in partial melts of amphibolite. In either case differentiation is dominantly in the mid-deep crust.

The signature of amphibole indicates that a significant H_2O-bearing reservoir exists in the arc crust, which may be tapped to produce silicic, explosive magmas or ore-forming fluids. Furthermore, amphibole has the capability of rotating REE patterns to obtain the characteristic light REE enrichment of the continental crust.

Construction of the ion nanoprobe: A progress report

A.M. DAVIS[1,2,4], I.V. VERYOVKIN[3,4], T. STEPHAN[1,4], M.J. PELLIN[3,4], M.R. SAVINA[3,4], R. PARAI[1,4], K.B. KNIGHT[1,4] AND J. LEVINE[1,4]

[1]Department of the Geophysical Sciences, University of Chicago, Chicago, IL 60637 (a-davis@uchicago.edu)

[2]Enrico Fermi Institute, University of Chicago

[3]Materials Science Division, Argonne National Laboratory, Argonne, IL 60439

[4]Chicago Center for Cosmochemistry

We report on progress towards construction of the ion nanoprobe, a new instrument designed for isotopic and chemical analysis at the few-nm scale [1]. The new instrument will combine a recently developed high resolution liquid metal ion gun (LMIG), tunable solid state lasers for laser resonant ionization, a molecular fluorine excimer laser for UV ionization, and an improved time-of-flight mass spectrometer. The instrument is intended to provide a significant decrease in spot size and increase in sensitivity compared to the current state-of-the-art SIMS instrument, the Cameca NanoSIMS-50: the LMIG can be focused to 10 nm; the most advanced previous generation of this type of instrument, SARISA, has recently demonstrated a useful yield (atoms detected per atom removed) of greater than 20% [2], and our goal is 35%. Isotopic precision is currently at the few permil level, as a result of a number of recent advances in laser position and wavelength stabilization [3]. Compared to SARISA, the ion nanoprobe will operate at significantly higher accelerating voltage, improving mass resolution and sensitivity, and will have a finer-focused primary ion beam. The physical layout will also be different, with the flight tube of the ion nanoprobe mounted vertically above the sample chamber; this assembly will be mounted in the center of an H-shaped laser table equipped with active vibration cancellation devices. A thermally stabilized, low-vibration, draft-free room to house the ion nanoprobe is now under construction.

Much of the cometary dust returned by the Stardust mission from Comet Wild 2 has been processed at high temperature and presolar grains like those found in meteorites and interplanetary dust particles are very rare. Contemporary interstellar grains collected by Stardust are just now being extracted and will be a high priority for the ion nanoprobe, as will be small presolar SiC and subgrains in presolar graphite that are beyond current analytical technology.

[1] Davis *et al*. (2007) *Geochim. Cosmochim. Acta* **71**, A205.
[2] Veryovkin *et al*. (2008) *Lunar Planet. Sci.* **39**, #2396.
[3] Levine *et al*. (2008) *Lunar Planet. Sci.* **39**, #1661.

Thermal models of incremental pluton emplacement

J.W. DAVIS AND D.S. COLEMAN

Dept. of Geological Sciences, University of North Carolina-Chapel Hill (davisjw@email.unc.edu)

Thermal modeling of pluton assembly via incremental addition of sheet-like intrusions yield the following general observations: 1) partial melting of wall rock is absent early in the history, but becomes more prevalent through time, 2) an amorphous zone of interconnected melt is formed independent of intrusion geometry, 3) melt percentages averaged over the assembled body are low, 4) temperatures cycle near the granitic solidus for protracted periods of time. In the models, early intrusions are emplaced into a cool geothermal gradient (relative to later intrusions) and quickly cool below the solidus. Later intrusions intrude into progressively hotter environments and remain at elevated temperature for longer times. We suggest that this progression from a rapidly to slowly cooled system may erase contacts between increments, promote megacryst growth, and yield a progression from simple to complex zircon systematics, and protracted cooling. Emplacement as small increments does not develop a zone of voluminous interconnected melt, instead the active magma body is only a small portion of the total volume intruded. Models are consistent with geophysical data from active magmatic zones that fail to image regions likely to contain more than 20% melt. Incremental emplacement precludes large-scale pluton convection, and as such, inhibits large-scale internal differentiation by magmatic processes. The incremental emplacement model may require a re-evaluation of connections between volcanism and plutonism. If plutons form from small episodic sheet-like intrusions and only develop minor zones of interconnected melt, the idea that plutons are sub-volcanic crystallized remnants of large volume ignimbrite eruptions may be problematic.

Near-equilibrium investigations of quartz and forsterite dissolution

M.C. DAVIS[1]*, D.J. WESOLOWSKI[2], L.M. ANOVITZ[2], L.F. ALLARD[2], S.L. BRANTLEY[3] AND K.T. MUELLER[1]

[1]Penn State University, Dept. of Chemistry, University Park, PA 16802 (*correspondence: mcd930@psu.edu) (ktm2@psu.edu)

[2]Oak Ridge National Lab, Oak Ridge, TN 37831 (wesolowskid@ornl.gov, anovitzlm@ornl.gov, allardlfjr@ornl.gov)

[3]Penn State University, Dept. of Geosciences, University Park, PA, 16802 (brantley@essc.psu.edu)

While many kinetic studies have focused on dissolution and precipitation reactions under far from equilibrium conditions, few studies have focused on the near equilibrium region. Recent studies of boehmite dissolution conducted by Bénézeth and coworkers [1] have used continuous pH monitoring at high temperatures to follow a reaction as it approaches equilibrium. We have used similar techniques to better understand the near equilibrium behavior of quartz and forsterite. Experiments were conducted at undersaturated and supersaturated conditions to look at both dissolution and precipitation kinetics. While dissolution was expected to follow a simple first order kinetic model, quartz studies at pH 8-10 and 125-200°C indicate a more complex dissolution mechanism not easily normalized by solution chemistry. Therefore, a more complex analysis of dissolution data has been undertaken. Nucleation theory was initially used to explain crystal growth but Dove [2] extended it to explain the kinetics of silicate minerals including quartz. Unlike quartz, understanding forsterite dissolution is complicated by incongruent magnesium-to-silicon release, leached layer formation, and the precipitation of a secondary magnesium-rich phase. Forsterite dissolution kinetics in acidic solutions cannot be followed with respect to silicon in the same manner as quartz since only $[Mg^{2+}]$ can be extrapolated from pH through charge balance. To identify a possible secondary phase and probe leached layer formation, solid-state nuclear magnetic resonance (NMR) has been used in conjuction with additional analytical techniques including wet chemical analysis, transmission electron microscopy, and x-ray and neutron diffraction. Here we present our studies of near equilibrium kinetics for quartz, as well as evidence of precipitate formation during forsterite dissolution.

[1] Benezeth, Palmer, & Wesolowski. (2007, submitted) *Geochemical et. Cosmochimica Acta.* [2] Dove, Han & Yoreo. *Proceedings of the National Academy of Sciences* **102**, 15357-15362.

In situ U-Pb dating of diagenetic apatite and xenotime: Paleofluid flow history within the Thelon, Athabasca and Hornby Bay basins

W.J. DAVIS*[1], R.H. RAINBIRD[1], Q. GALL[2] AND C.J. JEFFERSON[1]

[1]Geological Suvery of Canada, 601 Booth St. Ottawa, ON. K1A (0E8bidavis@nrcan.gc.ca)
[2]1864 Rideau Garden Drive, Ottawa, ON

Results of *in situ* ion probe dating of diagenetic fluorapatite and xenotime are reported for sandstones from the Paleoproterozoic Thelon, Athabasca and Hornby Bay intracontinental, uraniferous basins of northwestern Canada.

Diagenetic fluorapatite occurs at multiple stratigraphic levels within the Thelon and Athabasca basins as interstitial cements and in veins and breccias that cut across bedding. Fluorapatite occurs as euhedral, oscillatory-zoned crystals interpreted to have formed during mesogenesis. A previous U-Pb TIMS study of bulk apatite interpreted three discrete events within the Thelon Basin at 1.72, 1.68 and 1.65 Ga [1]. However, 52 *in situ* analyses from five samples, including a subset from the earlier study, define a single population with an age of 1.667 ± 0.006 Ga and no evidence of multiple depositional events. This age is older than the 1.64-1.61 Ga ages reported for the Athabasca Basin [2, this study] indicating independent fluid-flow histories and timing of fluorapatite cementation in the two basins. The drivers of the fluid-flow events are unknown but could include orogenesis in southern Laurentia (e.g. Mazatzal-Central Plains-Labradorian orogeny), or possibly mafic magmatism, evidence for which is preserved in upper part of the Thelon Basin.

Fluorapatite cement also occurs within the Hornby Bay Basin. U-Pb data yield a less precise age of 1.16 ± 0.08 Ga due to lower uranium contents. Localized xenotime cement, in corrosive contact with detrital quartz and early quartz cement, yields an age of 1.284±0.011 Ga. Phospate cementation is significantly younger than the depositional age but similar to a reported uraninite age of ~1.05 Ga [5]. Fluorapatite and xenotime cementation most likely occurred during a fluid-flow event driven by 1.267 Ga Mackenzie magmatic activity. Fluid-flow driven by regional magmatism is recognized in other Proterozoic basins [3, 4].

[1] Miller *et al*. (1989) *CJES* **26**, 867-880. [2] Rainbird *et al.* (2003) *SIR Open House*, 6. [3] Ray *et al*. (2008) this volume. [4] Rasmussen *et al.* (2007) *Geology* **35**, 931-934. [5] Triex Minerals Corp. – 43-101 report.

Cave-analogue calcite growth in the laboratory: Calibrating stalagmite palaeoproxies

C.C. DAY[1], G.M. HENDERSON[1] AND K.R. JOHNSON[1,2]

[1]Department of Earth Sciences, University of Oxford, UK (chris.day@earth.ox.ac.uk)
[2]Now at, University of California, Irvine, USA (kathleen.johnson@uci.edu)

An increasing number of studies report stable-isotope and trace-element records in speleothems. This variation is controlled by diverse environmental variables including the climatically important variables, temperature and rainfall. There is, however, a paucity of laboratory studies attempting to understand the influence of these environmental controls on stalagmite geochemistry. Quantitative data from such studies would dramatically improve our ability to reconstruct palaeoclimate from stalagmites.

We have completed a new series of carbonate growth experiments in karst-analogue conditions in the laboratory. The setup closely mimics natural processes (e.g. precipitation driven by CO_2 degassing, low ionic strenth solution, thin solution film) but with a tight control on growth conditions (temperature, pCO_2, drip rate, calcite saturation index and the composition of the initial solution).

Calcite is dissolved in deionized water in a 20,000 ppmV pCO_2 environment. Mg, Sr, Ba, Li, Na, U, Cd and Co are added to the initial solution, such that X/Ca is maintained constant between experiments. This solution is then dripped onto glass plates (coated with seed-calcite) in a lower pCO_2 environment (<2500 ppmV pCO_2). Experiments were performed at 7, 15, 25 and 35ºC. At each temperature, calcite was grown at three drip rates (2, 6 and 10 drips per minute), on separate plates within the same environment.

Oxygen isotope values are close to equilibrium given $\delta^{18}O_{solution}$ and temperature, but show small deviations from equilibrium, which are consistent with the relative drip rate and growth mass of the experiments. Trace metal relationships are also systematic with, for instance, Mg and Cd both showing relationships to temperature that are consistent with thermodynamic trends and demonstrating a predictable response to drip rate.

The integrated data provides significant new insight into the way that stalagmite carbonate responds to climatically important environmental variables.

Constraining deep mantle contributions to Canary Island lavas

J.M.D. DAY[1], R.J. WALKER[1], D.R. HILTON[2], J.-C. CARRACEDO[3] AND E. HANSKI[4]

[1]Dept. Geology, Univ. Maryland, College Park, MD, USA
[2]Scripps Institution of Oceanography, La Jolla, CA, USA
[3]Estación Volcanológica de Canarias, Tenerife, Spain
[4]Dept. Geosciences, Univ. Oulu, FIN-90014 Finland

Much debate surrounds the original interpretation of coupled ^{186}Os-^{187}Os enrichments in ocean island basalts (OIB) as deriving from core-mantle interaction. Alternate models proposed to explain ^{186}Os-^{187}Os signatures include melting of pyroxenite-peridotite mixtures, or base metal sulphides, with long-term (Re+Pt)/Os enrichment. Canary Island lavas offer a means to test these models because they are characterised by radiogenic $^{187}Os/^{188}Os$ and Pb isotopes, and MORB-like $^{3}He/^{4}He$ – characteristics which can be interpreted as originating from a predominantly upper mantle source that includes recycled crust/lithosphere, rather than a 'deep plume' component. We present new coupled high-precision ^{186}Os-^{187}Os isotope and highly siderophile element (HSE) abundance data on picrite and ankaramite lavas from the islands of El Hierro, La Palma, La Gomera, Tenerife, Lanzarote, and on harzburgite xenoliths from Lanzarote.

Lavas analysed in this study have 0.15 to 1.2 ppb Os, and $^{187}Os/^{188}Os$ ranging from 0.137 to 0.166. These ratios are at the extreme radiogenic range of OIB. The Os concentrations are similar to rocks with comparable MgO worldwide, so there is no evidence of derivation from an HSE-depleted source. The harzburgite xenoliths are characterised by >1 ppb Os, chondritic to sub-chondritic $^{187}Os/^{188}Os$ and Re depletion ages consistent with their origin as lithospheric refractory melt residues. $^{186}Os/^{188}Os$ data for three aliquots of a Lanzarote harzburgite yield a ratio of 0.1198361±9; indistinguishable from estimates for the convecting upper mantle. Analysed Canary Island lavas have $^{186}Os/^{188}Os$ ratios that are also within the upper mantle range.

The observation that $^{186}Os/^{188}Os$ of Canary Island lavas are typical of the upper mantle points to a lack of long-term Pt/Os enrichment, but the extreme range in $^{187}Os/^{188}Os$ indicates a source with long-term Re/Os enrichment. Combined, these characteristics are consistent with a mantle source containing variable proportions of recycled material within a peridotitic, depleted-MORB mantle. Such pyroxenite-peridotite, 'layer-caked' sources have been suggested as the cause of coupled ^{186}Os-^{187}Os enrichments in other OIB mantle sources. The new data obtained on Canary Island lavas do not appear to support this view.

Search of hydrocarbon in Mesozoic sediments below the Deccan basalt, India

A.M. DAYAL, D.J. PATIL AND S.V. RAJU

National Geophysical Research Institute Hyderabad 500 007, India (dayalisotope@yahoo.com)

The Cretaceous Deccan basalt is one of the larger and better-preserved continental flood basalt (CFB) provinces of the world (Fig.1). Based on DSS studies, Kaila (1988) indicate a hidden sedimentary basin trending E-W near Tapti River bound by E-W faults, named the Tapti graben, with its thickness of 1.8 km decreasing to 400 meters near Surat and Akola. To search the presence of hydrocarbon in hidden Mesozoic sedimentary basin below the Deccan basalt geochemical study of soil samples was carried out for the light hydrocarbon (C_1-C_4).

The light gaseous hydrocarbons were extracted from soil by treating sample with orthophosphoric acid. C_1-C_4 was measured using gas chromatograph. The accuracy of measurement of $C_1 - C_4$ components is < 1 ng/g. Carbon isotopic composition of $\delta^{13}C_1$ (methane), $\delta^{13}C_2$ (ethane) and $\delta^{13}C_3$ (propane) was measured using GC-C-IRMS. The precision of the isotopic analysis for CH_4 is ± 0.5‰.

The adsorbed soil gas analysis for Deccan Syneclise indicates that the concentrations of methane, ethane propane and butanes are moderate to low Fig 2a, 2b, 2c). The cross-plots (Fig. 3) between C_1-C_2, C_1-C_3, C_2-C_3 and C_1-ΣC_{2+} show excellent correlation (r = >0.9) and suggest that these hydrocarbons are genetically related not effected by secondary alteration during their migration from subsurface and have been generated from a thermogenic source because of the presence of C_2 & C_3 components. The compositional signatures displayed by methane to ethane (C_1/C_2), methane to propane ratios (C_1/C_3), as defined by Pixler (1969) is shown in Fig. 4, it can be seen that majority of the samples fall in oil window and oil & gas window.

The relationship between $\delta^{13}C_1$ and gas wetness $C_1/(C_2+C_3)$ indicates that majority of the samples fall within the thermogenic field (Fig. 5). The adsorbed soil gas data as well as $\delta^{13}C_1$ signatures suggest that the light gaseous hydrocarbons (C_1-C_3) are derived predominantly from thermogenic source.

The main objective of this work was to search the presence of hydrocarbon in the hidden basin of Mesozoic age below the Cretaceous Deccan basalt. The region in and around Upper Godavari lineament, Tapti graben and north of Tapti Graben indicate anomalous concentration of hydrocarbon gases.

No figures were submitted for publication in this abstract.

The age, duration, and depth of a turbulent magma ocean in Mars

V. DEBAILLE[1], A.D. BRANDON[2], Q.-Z. YIN[3] AND B. JACOBSEN[3]

[1]Lunar and Planetary Institute, Houston, TX 77058, USA now at Université Libre de Bruxelles, Brussels, Belgium (vinciane.debaille@ulb.ac.be)
[2]NASA-Johnson Space Center, Houston, TX 77058, USA (alan.d.brandon@nasa.gov)
[3]University of California Davis, Davis, CA 95616, USA (yin@geology.ucdavis.edu jacobsen@geology.ucdavis.edu)

One key aspect of early differentiation in terrestrial planets presently under debate is when did magma oceans (MO) form, how long did they last, and how deep were they? The heat released by accretion, short-lived radioactive elements, and core formation was likely sufficient to at least partially melt the silicate portions of terrestrial planets resulting in global-scale MO's. In order to investigate these issues for Mars, $^{142}Nd/^{144}Nd$, $^{143}Nd/^{144}Nd$, $^{147}Sm/^{144}Nd$, $^{176}Hf/^{177}Hf$ and $^{176}Lu/^{177}Hf$ data have been obtained on 9 shergottite meteorites. Shergottites fall along a mixing line between two distinct sources. This line does not pass through the chondritic point in ^{142}Nd-^{143}Nd systematics The mixing line is consequently not an isochron and this observation is independent of the initial Sm/Nd of Mars. The depleted end-member with high $^{147}Sm/^{144}Nd$ and $^{176}Lu/^{177}Hf$ is best represented by the depleted shergottites DaG476 and SaU008/094, and record differentiation ~35 Myr after solar system formation in their ^{142}Nd-^{143}Nd systematics. The enriched end-member with long-term subchondritic Sm/Nd, is preferentially sampled by enriched shergottites Zagami, Shergotty, Los Angeles, and NWA856. This end-member is likely to be late-stage quenched residual melt from the MO and differentiated ~100 Myr after solar system formation. This indicates an extended duration for the Martian MO, requiring an external process to slow down its crystallization rate, such as a primitive atmosphere acting as insulating blanket. In addition, the calculated Lu/Hf and Sm/Nd source ratios of depleted shergottites cannot be reproduced directly by cumulates crystallizing from the MO, but instead require a mixture between segregating crystals and residual melts. This is a direct consequence of turbulences in a convective MO. The Martian mantle source of depleted shergottites is the result of mixture between cumulates and ~2.5% of residual trapped melts. Finally, the Lu-Hf and Sm-Nd systematics in shergottites are consistent with a MO deeper than 1350 km.

High-Mg andesites from Glacier Peak WA, derivatives of mixing between low- and hi-Si endmembers

S.M. DEBARI[1], T.W. SISSON[2] AND D.D. TAYLOR[1]

[1]Geology Department, Western Washington University, Bellingham, WA (debari@geol.wwu.edu)
[2]U.S. Geological Survey, Menlo Park, CA (tsisson@usgs.gov)

Four small volume Quaternary mafic cinder cones and lava flows are present 5-10 km south of Glacier Peak, a dacitic stratovolcano in the northern segment of the Cascades magmatic arc. One of these flows, the Lighning Creek, consists of high-Mg basaltic andesite to high-Mg andesite (54.8-58 wt.% SiO_2) with Mg#s (100xMg/[Mg+Fe^T]) = 68-66, MgO = 7.8-6.3 wt.%, and 140-108 ppm Ni. The flow is isotopically heterogeneous, with ε_{Nd}=6.5-7.1; $^{87}Sr/^{86}Sr$=0.7030-0.7035; and $^{206}Pb/^{204}Pb$=18.77-18.81. The major, trace, and isotopic variations within this flow are inconsistent with fractional crystallization as the sole or dominant cause of compositional diversity. For example, Sr and La concentrations *decrease* with increasing SiO_2. Instead, chemical and isotopic trends are consistent with mixing with a Sr and La-poor felsic component, closely similar to dacites from nearby Glacier Peak (63-65 wt.% SiO_2, Mg# 47-51), to produce the high-Mg andesites of the suite. These dacites have more enriched isotope ratios than the andesites and basaltic andesites (ε_{Nd}=5.2; $^{87}Sr/^{86}Sr$=0.7036; and $^{206}Pb/^{204}Pb$=18.86), slightly higher La/Sm, but lower Dy/Yb and Sr/Y. Petrographic observations of disequilibrium textures such as xenocrysts, quenched glass inclusions, and strongly zoned and embayed phenocrysts support this conclusion of magma mixing.

All Lightning Creek samples have petrographic evidence for mixing, so the parental magma must have been less evolved (lower SiO_2) than the most primitive sample observed. Extrapolation of the mixing trend by modest amounts (removal of 10-20 wt.% dacite) predicts a parental magma composition near the basalt-basaltic andesite classification boundary. Similar relatively SiO_2-rich magnesian basalts and SiO_2-poor magnesian basaltic andesites are common elsewhere in the Cascades. Magnesian "true" andesites (SiO_2 56-62 wt.%) are not, and near Glacier Peak such magmas are products of mafic-felsic magma mixing.

Iron and trace elements cycling in mineralized paleolaterites from NW Tunisia

S. DECREE[1]*, TH. DE PUTTER[2], J. DE JONG[1], CH. MARIGNAC[3] AND J. YANS[4]

[1]Université Libre de Bruxelles, Department of Earth and Environmental Sciences, B-1050 Brussels, Belgium (*correspondence: sdecree@ulb.ac.be).
[2]Royal Museum for Central Africa, Dept. Geology, B-3080 Tervuren, Belgium
[3]G2R- Nancy Mining School, F-54000 Nancy, France
[4]Namur University, Dept. Geology, B-5000 Namur, Belgium

The Tamra (NW Tunisia) iron mine is composed of a 50m-thick series of stacked shallowing-upward sedimentary sequences. Iron is concentrated within these sequences by combined pedogenetic and hydrothermal processes. We used Fe isotopes (by MC-ICP-MS) and trace elements analyses (by ICP-MS) to constrain Fe and trace elements distributions in the typical sedimentary sequence (from top to bottom): massive hematite + quartz bar; goethite + hematite mixed horizon; kaolinite + hematite clayey level.

Our results indicate that: (1) There is an overall depletion of MREE, U and light iron (^{54}Fe) into the clayey term: Th/U ratios ranges from 3.5 to 5.2 and δ^{56}Fe from +0.79‰ to +1.07‰. (2) Within the intermediate hematite- and goethite-rich term, selected REE (La, Eu, Yb, Lu) are depleted, producing a typical tetrad effect in the REE patterns. By contrast, U and light iron are concentrated, most probably through adsorption onto pre-existing iron oxides. Th/U ranges from 0.4 to 1 and δ^{56}Fe from -1.03‰ to +0.34‰. (3) The lowermost massive bar acts as drain and partially concentrates the REEs percolating downward from underlying terms. A moderate U depletion and light iron accumulation are noted: Th/U ranges from 3.5 to 6.9 and δ^{56}Fe from -0.44‰ to +0.58‰.

These data suggest that pedogenesis results in a downward redistribution of REE, U and ^{54}Fe (or Fe^{2+}_{aq}) onto the lower terms where they are efficiently trapped by adsorption. Complexing agents are present in the system to mobilize the elements: hydrothermal sulphates and pedogenetic humic/fulvic acids. Although a non-null elemental budget in the type sequence suggests that it does not act as a closed system, there is actually internal (re-) cycling of the studied elements within "semi-closed" cells.

SD is a FNRS –FRIA grantholder.

Decoupling of Cu and As in Magmatic-hydrothermal systems: Evidence from the Pueblo Viejo Au-Ag deposit, Dominican Republic

A.P. DEDITIUS[1], S. UTSUNOMIYA[2], R.C. EWING[1] AND S.E. KESLER[1]

[1]Department of Geological Sciences,University of Michigan, Ann Arbor, MI 48109-1005 USA
[2]Department of Chemistry, Kyushu University, Fukuoka-Shi, 810-8560, Japan

Pyrite from the Pueblo Viejo high-sulfidation deposit provides evidence for decoupling of Cu and As in hydrothermal solutions. The pyrite that shows this decoupling is in the late-stage veins that also contain sphalerite and minor enargite. Pyrite in the veins shows growth zoning that varies in composition with depth into the deposit. Deepest veins (>150m below the present surface) contain fine-grained (<2□m) pyrite with 0.4% As, 0.5% Pb, 0.2% Cu, 0.1% Ag, 0.09% Te and 0.06% Sb (wt% by EMPA). At depths of 120-103m below the present surface, pyrite contains alternating growth zones with either Cu (<0.78%) or As (<0.69%), but never both. Farther upward in the deposit concentrations of Cu and As in the two types of pyrite increase and Pb (<1.8%), Sb (<0.33%), Ag (<0.1%) and Te (<0.08%) are also in As-rich zones. At a depth of ~20m, Cu and As reach concentrations of up to 3 wt% in separate, alternating growth zones. EMPA elemental maps of the shallowest pyrites reveal that increased concentrations of As and Cu coincide spatially with decreasing concentrations of Fe and show no relation to S, suggesting that both elements substitute for Fe. Chemical compositions of Cu-pyrite and As-pyrite are: $(Fe_{0.95}Cu_{0.06})_{1.01}S_2$ and $(Fe_{0.96}As_{0.05})_{1.01}S_2$, respectively. HRTEM observations on pyrite with highest Cu and As concentrations reveal that the pyrite consists of single crystals that are continuous from Cu-rich to As-rich growth zones. There is no visible (by TEM) grain boundary between Cu-rich and As-rich zones. Cu-rich growth zones contain no Cu-bearing inclusions, whereas As-rich growth zones contain numerous ordered nano-domains rich in As.

The alternating sequence of Cu-rich and As-rich zones appears to reflect separation of Cu from As during evolution of the hydrothermal fluids. Similar decoupling of As and Cu is seen in analyses of fumaroles and fluid inclusions (both vapor and liquid), which are enriched in As and Cu, respectively. This suggests that the decoupling is related to magmatic processeses, probably involving vapor-liquid transitions.

Magmatic evolution and distribution in the Taupo Volcanic Zone, New Zealand

C.D. DEERING[1]*, J.W. COLE[1] AND T.A. VOGEL[2]

[1]Dept. Geological Sciences, Univ. Canterbury, PB 4800, Christchurch 8020, New Zealand (*correspondence: cdd21@student.canterbury.ac.nz)

[2]Dept. Geological Sciences, Michigan State Univ., 206 Natural Sciences Bldg., East Lansing, Mi, 48824-1115, USA (vogel@msu.edu)

Evaluation of a large bulk-rock and mineral database of rhyolite from the Taupo Volcanic Zone (TVZ) provides important constraints on the evolution and distribution of these magmas through time and space. A range of compositions are observed and characterized by distinct differences in FeO*/MgO ratios, ASI, Ba/La, Y, and MREE. These differences reflect changes in the fH_2O, fO_2, P-T conditions in a 'hot zone' source region at the crust-mantle interface where these evolved melts are generated by fractionation/melting of successively emplaced basaltic magmas/plutons. Systematic variations in Y and MREE are consistent with variable proportions of amph/opx in the source, which reflect changes in P-T. A strong correlation between Ba/La and FeO*/MgO suggests fH_2O and fO_2 are also important in controlling the melt compositions.

The distribution of rhyolite magma compositions and melt production through time are governed by the central TVZ rift axis. Hydrous, more buoyant evolved-melts are generated at the lower crust-mantle interface directly below the central rift axis where the crust is thinnest. Subsequent melts are produced in a progressively higher P-T regime and are anhydrous. The duration and rate of melt production within these cycles are governed by the flux of H_2O released from the subducting slab, however, the distribution is governed by extension along the central rift axis.

Controls on As abundance in soils and sediments in Hawai`i

L.E. DE GELLEKE AND E.H DE CARLO

Department of Oceanography, SOEST, University of Hawaii Honolulu, HI 96822 USA

Although arsenic has been widely studied worldwide owing to its potential toxicity, fewer data exist for subtropical volcanic island settings. Several studies carried out in Hawai'i over the past decade examined trace elements in soils and sediments and produced a body of data, previously unavailable.

Our study was motivated by the fact that disagreement exists about the magnitude of natural background levels of As in Hawai'i and the consequent difficulty in defining "high concentrations". We have determined that soils and sediments contain trace natural concentrations of As of less than 20 ppm. Human activities, however, in particular the use of arsenical pesticides, have enriched certain soils and sediments, and As levels can reach several orders of magnitude above background [1, 3]. Arsenic-contaminated soils exist on large tracts of former sugar cane lands, where Cutler *et al*. [3] measured up to 1000 ppm As. Soil contamination has also been reported on other islands.

This presentation examines both the natural and anthropogenic controls on As distribution and occurrence in Hawaii soils and sediments and attempts to elucidate individual sources of this element. To date it appears that, in addition to the use crop pesticide, other anthropogenic sources of As in Hawaii include termiticides and certain fertilizers. Because the high topography and high rainfall (gradients) characteristic of Hawaii engender strong runoff and transport of materials, the distribution of As has been significantly altered through storm flow into selected water bodies.

[1] De Carlo, E.H., Beltran, V.L. & Tomlinson, M.S. 2004. *Applied Geochemistry*, **19(7)**,1011-1037. [2] De Carlo, E.H., Tomlinson, M.S. & Anthony, S.A. 2005. *Applied Geochemistry*, **20(12)**,2157-2188. [3] Cutler, W.G., Hue, N., Ortiz-Escobar, M.E. & Martin T. 2006. Proceedings of the 5th Int'l Conf. on Remediation of Chlorinated and Recalcitrant Compounds, B.M. Sass, Ed. (Battelle Press)

Pre- and post-accretionary carbonates in the Renazzo CR chondrite

B.T. DE GREGORIO[1]*, R.M. STROUD[1] AND D.S. EBEL[2]

[1]U.S. Naval Research Laboratory, Code 6366, 4555 Overlook Ave. SW, Washington, DC 20375-5320, USA (*correspondence: bradley.degregorio@nrl.navy.mil)
[2]American Museum of Natural History, New York, NY 10024-5192, USA

Although Renazzo and other CR chondrites have experienced extensive aqueous alteration [1], these meteorites also contain primitive organic matter [2]. We describe a reaction front boundary between pristine and aqueously altered matrix in a focused ion beam (FIB) extracted section by transmission electron microscopy (TEM) and synchrotron-based X-ray absorption near-edge structure spectroscopy (XANES). The altered portion of the section contains phyllosilicates, Fe-depleted pentlandite, and abundant elongated polycrystalline sulfide "slivers", while the pristine portion of the section contains well-rounded, discrete sulfides with no phyllosilicates. Organic matter and Ca-rich carbonates [3] are present throughout the section.

Combining Ca- and C-XANES with electron diffraction in the TEM, the carbonates are tentatively identified as aragonite ($CaCO_3$) and whewellite ($CaC_2O_2 \cdot H_2O$), which are difficult to distinguish based solely on composition. Ca-XANES is sensitive to changes in coordination (6-fold in calcite, 7-fold in whewhellite, and 9-fold in aragonite). Whewhellite spectra also include contributions from nearest-neighbor interactions with structural water.

Whewellite in the altered portion of the section is associated with organic matter and Fe-oxide, suggesting hydrous oxidation of organic matter and sulfide generation by parent body fluids. Carbonate in the pristine portion of the section, with no apparent interactions with surrounding matrix, may have formed by preaccretionary oxidation of primitive organic matter. Organic matter in the aqueously altered portion of the section appears to contain more oxidized moieties and less aromatic moieties than that in the pristine portion.

[1] Weisberg *et al.* (1993) *GCA* **57**, 1567-1586. [2] Busemann *et al.* (2006) *Science* **312**, 727-730. [3] Fredriksson *et al.* (1981) *Meteoritics* **16**, 316.

Geochemistry of mantle olivine and application to geothermometry

J.C.M. DE HOOG

Dept. of Earth Sciences, Oxford University, Parks Road, OX1 3PR, Oxford, UK (cees-jan@earth.ox.ac.uk)

Trace element compositions of olivines from 72 mantle rocks (xenoliths from kimberlites and basalts, orogenic peridotites) were analyzed to study systematic variations between mantle lithologies and rock compositions, partitioning mechanisms, and potential for geothermobarometry. Forsterite contents of the olivines fall between 89 and 93, whereas equilibrium P and T range from 800 to 1500°C and 15 to 75 kbar.

Trace elements in olivine can be divided into three groups. *Group 1 elements* (Ni, Mn, Co, Cu, Zn, Li) show a narrow range of concentrations and correlate with Fo content. Olivine is the major host for these elements. Except for Li, these are divalent elements with ionic radii close to that of Mg. *Group II elements* (Cr, Al, V, Sc, Ca, Na) show a large range of concentrations, mainly controlled by the equilibration temperature of the rock. They are strongly concentrated in co-existing mantle minerals (garnet, cpx, spinel) and have a narrow concentration range in the bulk rock. They fit less comfortably in the olivine lattice than Group I elements because of their charge or size. Differences between garnet and spinel-facies rocks are apparent for Al, V, and Sc. *Group III elements* (Ti, Zr, Nb, REE) show the largest range of concentrations, controlled mostly by bulk rock contents, and can thus be used to reconstruct melt depletion and metasomatic history of the host rock. They are strongly incompatible in olivine and other mantle minerals because of their charge and often size. Olivines from garnet, garnet-spinel and spinel-facies rocks can be distinguished using a Zr-Sc diagram.

Uptake of Al and Cr is charge-balanced by Na in *garnet-facies* olivine, with Al and Cr in about equal proportions, suggesting the presence of a $Na(Al_{0.5}Cr_{0.5})SiO_4$ component in olivine. In *spinel-facies* olivine a large excess of Al is present, which may be explained by uptake of Al via Tschermak-style substitution.

The temperature dependence of Group II elements can be used to express simple geothermometers solely based on the concentrations of these elements in olivine. The most promising of these is Al-in-olivine for garnet peridotites:

$T_{\text{Al-in-ol}}(K) = [12184 + 48.9P\,(kb)] / [14.61 - \ln \text{Al}_{\text{ol}}\,(ppm)]$

which predicts T within 20°C, is applicable to cpx-free harzburgites, and might, for example, be used to determine formation conditions of olivine inclusions and their host diamonds.

High-accuracy determination of Iron in Antarctic waters by isotope dilution MC-ICP-MS using nitrilotriacetic acid chelating resin for preconcentration and matrix separation

J.T.M. DE JONG[1]*, V. SCHOEMANN[2], D. LANNUZEL[1,3], J.-L. TISON[1] AND N. MATTIELLI[1]

[1]Université Libre de Bruxelles, DSTE CP160, Avenue F.D. Roosevelt 50, B-1050, Brussels, Belgium (*correspondence: jdejong@ulb.ac.be)
[2]Université Libre de Bruxelles, ESA CP221, Avenue F.D. Roosevelt 50, B-1050, Brussels, Belgium
[3]University of Tasmania, ACE-CRC, 80 Private Bag, Hobart, Tasmania 7005, Australia

In the present study, we propose a robust and simple method to measure dissolved iron (DFe) concentrations in seawater down to <0.1 nM level, by Isotope Dilution Multiple Collector Inductively Coupled Plasma Mass Spectrometry (ID-MC-ICP-MS) using a ^{54}Fe spike and measuring the ^{57}Fe/^{54}Fe ratio. The method consists of a pre-concentration step (100:1) on micro-columns with the resin NTA Superflow, of 50 mL seawater samples acidified to pH 1.9, at which pH the resin is demonstrated to quantitatively extract Fe. Blanks are low: grand mean 0.047 ± 0.020 nM (n = 18), detection limit (3SD) per session 0.020 – 0.069 nM range, because no buffer is required to adjust the sample pH for optimal extraction, and only ultrapure nitric acid, dilute H_2O_2, and acidified milli-Q water are needed. We measure SAFe reference seawater samples Surface-1 (0.121±0.029 nM, n=6) and Deep-2 (0.925±0.059 nM, n=8) and confirm their assigned consensus values. To demonstrate the feasibility of the method we present vertical DFe profiles from the western Weddell Sea and from the western Bellingshausen Sea, collected respectively during the ISPOL (2004/5) and SIMBA (2007) ice drift time series. At SIMBA, profiles exhibit variability in the upper mixed layer between 0.2 nM and 1 nM in the vicinity of melting icebergs, nutrient type behavior with deep water concentrations of 0.6-1.2 nM and bottom water enrichment up to 1.6 nM. At ISPOL, DFe in the upper mixed layer was 0.6 nM, in deep water 2 nM, with close to the bottom 23 nM. Bottom water enrichment arises from diagenetic Fe diffusion or sediment resuspension.

Origin of the 26-25 Ma flood basalts from Mont Havergal, northermost Kerguelen (South Indian Ocean)

G. DELPECH[1], F. NAURET[2], M. MOULIN[2], F. DESCHAMPS[3] AND J.Y. COTTIN[4]

[1]UMR IDES 8148 “Interaction et Dynamique des Environnements de Surface”, Univeristé Paris Sud-XI, 91405 ORSAY (guillaume.delpech@u-psud.fr)
[2]IPGP, Laboratoire de Géochimie-Cosmochimie and Laboratoire de Paléomagnétisme , 4, place Jussieu, 75252 PARIS Cedex 5 (nauret@ipgp.jussieu.fr, moulin@ipgp.jussieu.fr)
[3]LGCA, Université Joseph Fourier, 1381, rue de la piscine, 38400 Saint Martin d’Hères, France
[4]UMR 6524 “Magmas et Volcans”, Université Jean Monnet, 23, rue du Dr. Paul Michelon, 42023 SAINT-ETIENNE, France (jean.yves.cottin@univ-st-etienne.fr)

Mont Havergal is a 550 m section of flood basalts situated at the northernmost part of the Kerguelen Archipelago (South Indian Ocean). Available Ar/Ar dating of flood basalt sections in the northern part of the Kerguelen Archipelago range between 30 and 28 Ma. K/Ar dating using the Cassignol-Gillot technique indicate that the Mont Havergal flood basalts erupted between 26.4±0.4 Ma and 25.2±0.4 Ma and are therefore significantly younger. The 22 flows analysed are basalts of transitional affinity, except for the occurrence of a more evolved lava flow in the middle of the section with a trachy-andesitic composition. These flows display a wide range of trace element contents and trace element ratios such as for La/Sm or Dy/Yb. Some have trace element contents and ratios that are close to those of Indian MORBS, whereas others have ratios typical of OIB magmas from the Kerguelen plume. Other flood basalts that erupted at the same time on the Archipelago, located mostly in the central part of the main island, reflect the contribution of plume melts (^{87}Sr/^{86}Sr=0.7046-0.7052 and ^{143}Nd/^{144}Nd=0.51272-0.51258). Contrarily, the Mont Havergal basalts are much more variable in terms of trace elements and Sr-Nd isotopic compositions (0.7042-0.7056 and 0.51282-0.51246). Some isotopic compositions reflect a strong contribution from a depleted mantle source (Indian MORB) while others an enriched mantle source with a more extreme composition than that inferred for the Kerguelen plume. The data suggest that the plume may have been zoned or that plume-ridge interactions were still taking place, although the SEIR was about 700 km away from the plume.

Tracing ore forming fluids of gold deposits hosted in Kangding complex in Sichuan province, China

J. DENG[1]*, Q. GONG[2], Q. WANG[2], L. YANG[2] AND Z. ZHANG[2]

[1]State Key Laboratory of Geological Processes and Mineral Resources, China University of Geosciences, Beijing, 100083, China (*correspondence: djun@cugb.edu.cn)

[2]Faculty of Earth Sciences and Resources, China University of Geosciences, Beijing 100083, China

Daduhe River ore belt in Sichuan province is an important gold belt in China. Most gold deposits in this belt locates in Kangding complex, which mainly consists of dioritoids, granitoids and amphibolites. Three gold deposits of Sijiazhai hosted in amphibolite, Guitaizi in Granite, and Taogou in the contact belt of Granite and amphibolite were selected to trace ore forming fluids. Because the altered host rocks of ore body resulted from the interaction between host rocks and ore forming fluids, we compared the REEs and $\delta^{34}S$ data (Table 1) in host rocks and altered host rocks to trace ore forming fluids.

Deposits	Host Rock	δEu		$\delta^{34}S$
		HR	AHR	Py (Cpy)
Sijiazhai	**Amphibolite**	**1.17**	**0.66**	**0.1 (2.3)**
Guitaizi	**Granite**	**0.73**	**0.52**	**3.5**
Taogou	**Granite**	**0.57**	**0.30**	**5.7**

Table 1: δEu and $\delta^{34}S$ in gold deposits.

HR: Host Rock, AHR: Altered Host Rock, Py: Pyrite, Cpy: Chalcopyrite; $\delta Eu=Eu_N/(Sm_N \cdot Gd_N)^{1/2}$ and normalized by chondrite from Boynton (1984).

REE patterns normalized by chondrite are similar in shape except δEu in each pair rocks listed in Table 1. δEu values in altered rocks were lower than those in unaltered rocks manifestily. $\delta^{34}S$ values of sulfides in each deposits were near those in the magmatic sulphur isotope reservoir. These indicated that ore forming fluids maybe resulted from felsic magmatic fluids in deep source.

The increasing trend of $\delta^{34}S$ from Sijiazhai, Guitaizi to Taogou gold deposits with the decreasing trend of δEu in Table 1 indicated deep source ore forming fluids were mixed with crust matters.

MIRA: A new high sensitivity, multicollector mass spectrometer for isotopologue and ultra-small sample stable isotope analysis

P.F. DENNIS

Stable Isotope Laboratory, School of Environmental Sciences, University of East Anglia, Norwich NR4 7TJ, UK (p.dennis@uea.ac.uk)

The recent development of isotopologue (isotopic cluster) measurements in natural materials is pushing against the performance envelope of current instruments in terms of sensitivity, stability and high vacuum performance. For example, the most common of the rare isotopologues of the CO_2 molecule at m/z = 47 ($^{13}C^{18}O^{16}O$) has a natural abundance of just 44ppm and for useful palaeotemperature estimates it's relative concentration needs to be measured to a precision of 0.005‰, or better.

MIRA is a new stable isotope ratio mass spectrometer designed specifically for measurements of isotopologue species of the CO_2 molecule. It is based on a 25cm, 120° magnetic sector, with a symmetric extended geometry, stigmatic focussing and a dispersion of 50cm. The analyser is differentially pumped using drag stage turbopumps backed by diaphragm roughing pumps to ensure a completely hydrocarbon free vacuum. The detector array consists of 6 individual, deep faradays alligned with m/z = 44, 45, 46, 47, 48 and 49 and operating with a mass resolution of 250. The gain for each channel is 10^7 (m/z = 44), 10^9 (m/z = 45, 46), 10^{11} (m/z = 47) and 10^{12} (m/z = 48, 49). The ion source, based on the Nier electron impact design, operates at 10keV ion energy, has two-stage ion extraction, and an overall sensitivity of better than 1 ion per 200 CO_2 molecules.

This increased sensitivity coupled with a novel gas dual-inlet system with a constant pressure variable micro-volume on the sample side allows high sensitivity analysis of ultra-small samples (<0.5 bar μL of CO_2) for $\delta^{13}C$ and $\delta^{18}O$.

In testing we have run the instrument with a major beam signal of 5 x 10^{-7}A and a m/z = 47 signal of 2 x 10^{-11}A (=1.25 x 10^8 ions.s^{-1}). Using 50 sample-reference gas comparisons with a total run time of 30 minutes the standard error of the 47/44 ratio is better than 0.005‰. These results were obtained with 500 bar μL of cylinder CO_2, equivalent to a 2.5mg carbonate sample.

We are currently assessing the effect of source tuning, notably the source pressure, ionisation energy, and extraction geometry on the measured 47/44 ratio, and beginning to make measurements on CO_2 derived from carbonate mineral samples.

Regional isotopic patterns in granitic rocks of southern Tibet and evolution of crustal structure during the Indo-Asian collision

D.J. DEPAOLO[1], K.L. WEAVER[1], X. MO[2], Z. ZHAO[2] AND T.M. HARRISON[3]

[1]Dept. Earth and Planetary Science, Univ California, Berkeley, CA 94720-4767
(*correspondence: depaolo@eps.berkeley.edu)
[2]School of Earth Science and Mineral Resources, China University of Geosciences, Beijing 100083
[3]Institute of Geophysics and Planetary Physics, UCLA, Los Angeles CA 90095

Southern Tibet hosts one of the largest and youngest examples of a continental-margin composite granitic batholith, the Gangdese Batholith. This batholith is no longer geographically at a continental margin, and there are questions about how it relates to subduction as opposed to intra-crustal melting. Crystallization ages extend from Cretaceous to Miocene; much of the batholith probably formed at 45-55 Ma. We have begun a study of regional patterns in the Nd, Sr, Hf (zircon) and Pb isotopic compositions of the granitoids north of the Indus-Yalu suture (IYS) to investigate the relationship of magmatism to collision, the extent of mantle magma generation, and the age structure of pre-batholithic Tibetan crust. Granitoids in a N-S traverse near Lhasa show a gradient in ε_{Nd}, with mantle-like values adjacent to the IYS (+2 to +6) and much lower values (-5 to -14) at 80 to 120 km north. This type of spatial gradient in ε_{Nd} is found in other continental margin batholiths—(e.g. Sierra Nevada and Peninsular Ranges in California)—that are associated with subduction but not continental collision. Positive ε_{Nd} values usually indicate granitoids formed in oceanic crust with sedimentary cover. There is a 60 km-wide zone north of the IYS where this type of crust hosted the batholith even though the magmatism occurred after the beginning of collision. Decreasing ε_{Nd} northward indicates a decreasing ratio of mantle input/crustal assimilation due to progressively thickened crust. A discontinuity at about 29.8N latitude (just N. of Lhasa) may be the southern edge of pre-collision Tibetan basement. Miocene granites near the IYS have lower ε_{Nd} than older granites, suggesting crustal thickening and structural rearrangement by Miocene time. Peraluminous (2-mica) granites north of 30.0N latitude have ε_{Nd} of -7 to -14, corresponding to basement model ages of 1.2 to 1.8 Ga. More detailed regional isotopic characterization of the granites could help document both the initial crustal structure of southern Tibet and its tectonic and magmatic modification during collision.

Volcanism of the Bureja-Jiamusy superterrane as a reflection of a subduction setting evolution

I. DERBEKO

Institute of Geology and Nature Management FEB RAS, Blagoveshchensk (derbeko@mail.ru)

The Bureja-Jiamusy superterreane is supposed to be a fragment of the Gondwana land accretted to the Sino-Korea craton in the Late Permian [2] and in the Late Jurrassic, after the closure of the Mongolian-Okhotsk Ocean they formed a single whole with Siberia [3]. But paleomagnetic data [1] indicate that the width of the Mongolian-Okhotsk Ocean has been 3000 m before the Late Jurassic. At present the three coeval Late Mesozoic volkanic complexes of andesite formation of calc-alkali series were identified in the territory of the Northen Flank of the superterreane. I – (120-105 Ma): the rocks are from highly to moderately magnesian; moderately titaniferous; Sr (up to 1029 ppm), Nb (<4-10 ppm), Ta (0.49 ppm), (Eu/Eu*=0.89-1.05), (La/Yb)n=5.4-6.9, La/Ta=30-61, Sr/Y=36-47. II – (116-105 Ma): moderately magnesian and titaniferous, Sr (230-910 ppm), Zr (121-301 ppm), Hf (178-212 ppm), Nb (<5-13 ppm), Ta (0.39-0.72 ppm); (Eu/Eu*=0.74-0.85); (La/Yb)n=5.1-11.22, La/Ta=30-61, Sr/Y=24. III – (116-105 Ma): moderately magnesian, high titaniferous; Rb (43-135 ppm), Sr (190-642 ppm), Zr (129-412 ppm), Hf (3-13 ppm), Nb (7-39 ppm), Ta (1.36-1.90 ppm), Sr/Y=5-12, Eu/Eu*=0.99-0.56, (La/Yb)n=4.40-14.02, La/Ta=18-23. About 120 Ma ago the formation of volcanics with geochemical characteristics typical for products of subduction settings began throughout the whole territory of superterrane's northern flank. 111 Ma a magmatic activity shifted towards the margins of the northerh (II) and eastern (III) flanks (in modern coordinates) of the study superterrane. Volcanism loses the features typical for the subduction rocks: Sr concentration decreases, whereas the concentration of Nb, Ta, Rb, K increase. The rocks of the three complexes formated by peridotite melting. The K_{REE} =2.5-4.3; the ratios of incoherent elements (Ce, Zr, Nb, Th, Yb to La) are close to the constant values. The rocks of those complexes belong to the common magmatic process and its products are evolved due to a subduction waning within the study region. Basing on geohemical characteristic of the rocks from the Bureja-Jiamusy superterreane we established that a subduction tectonic scenario began to develop there about 120 Ma ago and it completed 105 Ma ago. At that time the superterreane was most likely either a separate structure or, at least, an active continent margin.

[1] Kravchinsky V.A., Cogne J.-P., Harbert W. & Kuzmin M.I. *Geophys. Journal Int*. (2002) **148**, 43-57. [2] Wilde S.A. & Wu F. *//Gondwana Research*. (2001) **4**, 46. P.823-824. [3] Zhao X., Coe R.S., Gilder S.A. & Frost G.M. *Australian Journ. Earth Sci.* (1996) **3**, 643-672.

The origins of the short-lived radionuclides in the solar system

S.J. DESCH

School of Earth and Space Exploration, Arizona State University, PO Box 871404, Tempe AZ, 85287-1404

In my keynote address, I will review the astrophysical origins of the short-lived radionuclides (SLRs) inferred from meteorites to have existed in the early Solar System. These include ^{41}Ca, ^{36}Cl, ^{26}Al, ^{60}Fe, ^{10}Be, ^{53}Mn, ^{107}Pd, ^{182}Hf, and ^{129}I, ranging in half-life from 0.1 to 16 Myr. In broad brush, the three possible sources can be termed inheritance, irradiation, and injection. Inheritance is possible if the molecular gas from which the Solar System formed happened to contain high abundances of an SLR. This requires the SLR be relatively long-lived (tens of Myr) to avoid decay, and inheritance of ^{60}Fe seems ruled out. A unique exception is ^{10}Be; a high fraction of Galactic cosmic rays are themselves ^{10}Be nuclei and can become trapped in the molecular cloud during collapse. Irradiation refers to production of SLRs within the Solar System by energetic ions accelerated in solar flares. Production and incorporation of SLRs into meteoritic components, in the observed proportions, is a modelling challenge, and is not possible for ^{60}Fe. Injection of SLRs by a stellar nucleosynthetic source is required to explain the presence of ^{60}Fe in the early Solar System. The only source naturally associated with forming solar systems is a core-collapse supernova; but over 50% of Sun-like stars do form in association with a supernova. A supernova is capable of injecting all of the known SLRs (except the unique ^{10}Be), in very nearly their observed proportions. I will review a variety of models pertaining to the inheritance, irradiation and injection scenarios.

Exploring for photosynthesis in deep time and space

D.J. DES MARAIS

NASA Ames Research Ctr., Moffett Field, CA 94035, USA

The rise of photosynthesis led ultimately to an energy source substantially exceeding the geochemical source from redox reactions associated with weathering and hydrothermal activity. Today, hydrothermal sources deliver (0.1-1) x 10^{12} mol yr^{-1} globally of reduced S, Fe^{2+}, Mn^{2+}, H_2 and CH_4; estimated to sustain about (0.2-2.0) x 10^{12} mol C yr^{-1} of organic C production by chemotrophs. Photosynthetic global productivity is about 9,000 x 10^{12} mol C yr^{-1}. Because oxygenic photosynthesis provides abundant reductant by splitting H_2O, it frees the biosphere from depending solely upon geochemical sources of reductants, e.g., hydrothermal and weathering processes.

Photosynthetic microbes created robust fossil records in part because they populated stable continental platforms and margins and thereby contributed to sediments having high potential for preservation. Proterozoic cyanobacterial fossils and organic biomarkers are well documented. Sedimentary steranes extend evidence of oxygenated environments into the Archean. Low $^{13}C/^{12}C$ values of some 2.8 Ga kerogens have been attributed to methanotrophic bacteria, which require O_2 and CH_4. Perhaps reduced C and sulfides in extensive platform and margin deposits are the most enduring legacies of photosynthesis.

There are hints of even earlier origins. The 3.43 Ga Strelley Pool cherts, W. Australia, show that diverse stromatolites populated a partially restricted, low-energy shallow hypersaline basin. Molecular studies of extant bacteria hint that the earliest chlorophyll-using photosynthesizers needed geochemical sources of reductants. Did these anoxygenic phototrophs once sustain an extensive, highly productive biosphere? Perhaps the substantial decline in geothermal activity during the Archean created a driver for the development of oxygenic photosynthesis. Can we further document the Archean biosphere? Will Mars exploration extend our understanding of emerging biospheres to even earlier times?

The stable Si isotope composition of eastern Atlantic Ocean seawater

G.F. DE SOUZA[1]*, B.C. REYNOLDS[1], J. RICKLI[1], M. FRANK[2] AND B. BOURDON[1]

[1]ETH Zurich, Institute of Isotope Geology and Mineral Resources, Switzerland (*correspondence: desouza@erdw.ethz.ch) (reynolds@erdw.ethz.ch rickli@erdw.ethz.ch bourdon@erdw.ethz.ch)

[2]IFM-GEOMAR, Leibniz Institute of Marine Sciences at the University of Kiel, Germany (mfrank@ifm-geomar.de)

We have analysed the stable isotope composition of dissolved silicon (Si) in seawater samples from the eastern Atlantic Ocean. These samples were collected on board the R/V *Polarstern* during cruise ANT XXIII/1 and have been analysed by high-resolution MC-ICPMS (*NuPlasma 1700*). The stable isotope composition of silicon is reported as $\delta^{30}Si$ in the standard delta notation of deviations in the $^{30}Si/^{28}Si$ ratio from the standard reference material NBS 28.

Deepwater $\delta^{30}Si$ (>2000m water depth) varies between water masses and increases both from south to north as well as upward in the water column, which appears to reflect mixing of an isotopically light southern water component with a heavier northern component. The linear mixing trend of $\delta^{30}Si$ against 1/[Si] in the deepwaters ($r^2 = 0.97$) indicates that the northern component endmember has a $\delta^{30}Si$ value of +1.5‰ to +1.7‰.

Thermocline waters show an upward increase in $\delta^{30}Si$ to values in excess of +2‰. Isotopically heavy values in near-surface waters are produced by the biological fractionation of Si isotopes by diatoms [1]. Estimates of the fractionation factor ε related to this utilisation based on both Rayleigh-type and steady-state ("multi-box" [2]) models are significantly lower than the experimentally determined value of -1.1‰ [1]. This discrepancy could be due to vertical mixing or lateral advection of waters that reduces the gradient of $\delta^{30}Si$ with depth in the water column.

[1] De La Rocha C. L. *et al.* (1997) *GCA* **61**, 5051-5056.
[2] Cardinal D. *et al.* (2005) *Glob. Biogeochem. Cyc*. **19**, doi: 10.1029/2004GB002364.

Epidote forming reactions in calc-alkaline rocks monitored by trace elements

MATHIAS DESSIMOZ[1]*, O. MÜNTENER[1], O. JAGOUTZ[2] AND D. HUSSEIN[3]

[1]Institute of Mineralogy and Geochemistry, Anthropole, CH-1015 Lausanne (*correspondence: mathias.dessimoz@unil.ch)

[2]Massachusetts Institute of Technology, 77 Massachusetts avenue Cambridge, ma 02139-4307

[3]Pakistan Museum of Natural History, Islamabad, Pakistan

Epidote is a common magmatic mineral in intermediate plutonic rocks. Experiments performed at different pressure establish a minimum pressure of crystallisation of epidote around 0.3-0.7 GPa depending mainly on bulk composition and on oxygen fugacity. However, few data are available on epidote stability in gabbroic rocks at H_2O-undersaturated conditions and in volcanic dykes.

Rare examples of epidote phenocrysts known in volcanic rocks of dacitic to rhyodacitic composition show complex and fine oscillatory zoning as well as many dissolution and recrystallisation features. 3D images, performed with micro-X-Ray tomography, show that the core of the phenocryst is often composed by a nucleation centre associated with a complex irregular zoning pattern. Relics of quartz in the core and the vermicular aspect of the zoning resemble to what could be observed in epidote found in plutonic rocks.

Magmatic epidote in mafic rocks is widespread in the lower part of the Kohistan Arc Complex in Northern Pakistan. The Jijal Complex is one of the few places in the world with epidote bearing mafic plutonic rocks in a K-poor natural system and to understand the phase relations involving epidote in gabbroic rocks. Epidote occurs as primary phase in garnet hornblende bearing gabbros and in some pegmatites together with quartz, rutile and paragonite. Preliminary trace element geochemistry demonstrates important variations in epidote. In the core, the pattern shows a strong enrichment in LREE compared to HREE ($(La/Yb)_N$ =14.8) with a large positive europium anomaly (Eu* = 5.3) whereas the trend in the rim is rather flat ($(La/Yb)_N$ =1.1) or even depleted in LREE ($(La/Yb)_N$ =0.29) with a weak europium anomaly (Eu* = 1.6). We will present chemical and oxygen stable isotope data on epidote bearing pegmatites to constrain the composition of interstitial liquids in mafic systems at high pressure.

A combined LA-ICP-MS and DEGAS study on Bediasites and Ivory Coast tektites

A. DEUTSCH[1], F. LANGENHORST[2,3], S. LUETKE[1] AND J. BERNDT[4]

[1]Institut f. Planetologie, Univ. Münster, D-48149 Muenster, Germany (*correspondence: deutsca@uni-muenster.de)
[2]Bayerisches Geoinstitut, Univ. Bayreuth, D-95440 Bayreuth, Germany (falko.langenhorst@uni-bayreuth.de)
[3]Institut f. Geowissenschaften, Univ. Jena, D-07749 Jena, Germany
[4]Institut f. Mineralogie, Univ. Münster, D-48149 Muenster, Germany (jberndt@uni-muenster.de)

Impacts processes yield different types of mineral and rock melts which after cooling/quenching occur as "impact glass" in different geological settings in, around, and far off an impact crater. To the latter group belong the tektites whose formation process is still not well constrained despite intense geochemical studies [1] and modeling attempts [2].

We have analyzed two Ivory Coast (IVC) tektites (source crater Lake Bosumtwi, Ghana) and three Bediasites (North American tektite strewn field, related to the Chesapeake Bay structure, Virginia). Electron microprobe (5 µm defoc. beam) major element, and LA-ICP-MS trace element analyses (spot diameter 60 µm) point to a remarkable homogeneity of the tektites, internally as well as the whole group. Any hint of a diffusive loss of certain elements (i.e., the more volatile ones) is absent. The glasses are exceptionally dry: DEGAS analysis yield an H_2O content of 20-30 ppm for Bediasites which contain in addition traces of CO. The IVC tektites are likewise extremely depleted in gases, they contain ~100 ppm H_2O, and traces of CO_2 and CO with $CO/CO_2 > 1$.

The presence of reduced species (CO, total lack of ferric iron), and the extremely low volatile content foster the conclusion that material now forming tektites must have experienced flash heating at extreme temperatures under highly reducing conditions followed by fast quenching. The chemical homogeneity probably reflect more the melt/ejection process than homogeneity of the precursor materials.

[1] Koeberl, C. (2007) In *Treatise of Geochemistry* online edition, Elsevier, 1.28.1 to 1.28.52 [2] Artemieva, N. (2008) *LPSC* **39**, abstract # 1651

Using a mechanistic adsorption model to understand the influence of soil pH on the environmental availability of Phosphorus: Application to a Chromic Cambisol

N. DEVAU, F. GEARD, E. LE CADRE, L. ROGER, B. JAILLARD AND P. HINSINGER

Biogéochimie du Sol et de la rhizosphère, UMR 1222, INRA, SupAgro, F-34060 Montpellier (devau@ensam.inra.fr)

Geochemical processes, particularly adsorption/ desorption, which control inorganic phosphorus (P) soil availability were affected by plant rhizospheric functions. In this study, we intended to characterize the influence of pH variations which occurred in rhizosphere on process controlling P availability. We used an approach combining chemical extractions and geochemical modelling to study the speciation of P in Mediterranean chromic cambisol soils. First, one dataset where soil pH was adjusted manually ranging from acidic to alkaline conditions (pH ≈ 3 to 10) were used. In second, three sub-samples were chosen and soil pH was modified by wheat growth with NO_3^- applications. All the samples were analysed with $CaCl_2$ extractions which is equivalent of aqueous P. We used the CD-MUSIC model in attempt to simulate P sorption based on $CaCl_2$ extracts.

For the first dataset, the fit between simulated and measured P-$CaCl_2$ was quite good (R^2 = 0.80 and RMSE = 0.034 mg kg^{-1}). This suggest that P available was controlled by sorption process in the soils studied [1]. The adsorption capacity of minerals and P surface complexes, both explained P-$CaCl_2$ variations as a function of pH. Modelling of the second dataset showed us that the increase of P-$CaCl_2$ in soils with plants was not fully explained by pH, we also need to consider citrate exudation. This model must be validated on other P-deficient soils.

[1] Gustafsson J.P. (2001) *European Journal of Soil Science* **52,** 639-653.

Plume-ridge interaction: Dying from the feet up

C.W. DEVEY[1] AND N. STRONCIK[2]

[1]IFM-GEOMAR, Wischhofstr. 1-3, D-24148 Kiel, Germany
[2]GeoForschungsZentrum Potsdam, Telegrafenberg, D-14473 Potsdam, Germany

Intraplate melting anomalies ("plumes") appear to affect mid-ocean spreading axes over large distances, leading to changes in the composition of the axial magmas and thickening of the oceanic crust. Despite the importance of such plume-ridge interaction for plate production, there is no concencus on how or in what form material transfer from plume to ridge occurs. More problematic still, the compositions of the plume magmas also change, becoming more mid-ocean ridge-like as the plume approaches the ridge. Explaining this in terms of a mutual exchange of material between plume and ridge is difficult in a system characterised by strong focussing of mid-ocean ridge magmas to the narrow spreading axis. We will present a model based on major and trace element and isotopic (Sr, Nd, Pb, Ne) compositions of the Pacific Foundation Seamount Chain and adjacent Pacific-Antarctic spreading axis which explains these two apparently incompatible observations as facets of the same interaction between the cylindrical melting zone of the upwelling mantle diapir and the tent-shaped melting zone beneath the spreading axis. The model´s predictions can be tested using observations from near-ridge hotspot chains around the world.

A new precise calibration of the Na/K geothermometer using a world database of geothermal fluids and improved geochemometric techniques

L. DÍAZ-GONZÁLEZ[1] AND E. SANTOYO[2]*

[1]Centro de Investigación en Energía, UNAM, Posgrado en Ingeniería (Energía) Privada Xochicalco s/n, Temixco, Mor., México 62580 (ldg@cie.unam.mx)
[2]Centro de Investigación en Energía, UNAM, SE-Geoenergía, Privada Xochicalco s/n, Temixco, Mor., México 62580 (*correspondence: esg@cie.unam.mx)

Temperature estimates of *Na/K* geothermometers can be inconsistent due to errors in calibrations, coefficients and chemical analyses. Differences are still observed between measured and predicted temperatures of geothermal wells. In light of these uncertainties, a new improved *Na/K* geothermometer has been developed. A new GEOthermal Fluid Database (GEOFD) was created using downhole temperature measurements and fluid compositions of wells from a wide variety of world geothermal fields. A total of 645 samples were compiled and evaluated by calculating ion charge balances (ICB), which enabled to select data with ICB<10% for a better geothermometer calibration. 380 samples were selected and re-evaluated for the detection of outliers in iterative ordinary linear regressions (*log Na/K* versus *1/T*) using combined geochemometric methods. Due to the size of GEOFD (n=380), the outlier detection was recursively examined by computing *studentized residuals*, which were analyzed as univariate data with 14 statistical discordant tests instead of bivariate discordant tests (which are only recommended for n<100). 38 outliers were detected to obtain a final structure of GEOFD with 342 samples. From this structure, 239 samples (70 %) were randomly taken out to derive the new geothermometer equation and the remaining 103 samples (30 %) were used for validation and comparison purposes. The new improved Na/K geothermometer (n=239) is given by the following equation:

$$t^{o}C = \frac{876.3(\pm 26.26)}{\log\left(\frac{Na}{K}\right) + 0.8775(\pm 0.0508)} - 273.15$$

where the numbers in parentheses are the coefficient errors; and *Na* and *K* are concentrations (in ppm). This new equation was succesfully validated and applied to estimate subsurface temperatures in 103 geothermal samples, which showed a much better agreement with the measured well temperatures, than those predictions provided by all the previous *Na/K* geothermometers developed for the geothermal industry.

Focused melt flow in the shallow mantle: Evidence for transient instabilities in the partially molten mantle beneath an ocean ridge?

H.J.B. DICK, B.E. TUCHOLKE AND M.A. TIVEY

Dept. of Geology & Geophysics, Woods Hole Oceanographic Institution, Woods Hole, MA 02543, USA (hdick@whoi.edu)

The Kane Megamullion is an oceanic core complex in the western rift mountains of the Mid-Atlantic Ridge at 23°30'N bordered by the Kane F.Z. exposing 2.2-3.3 Ma crust extending up to ~50 km wide along isochrons. This corresponds to nearly the entire length of a second order magmatic ridge segment – generally believed to be the fundamental unit of accretion at a slow spread mid-ocean ridge. Crust of corresponding age and position on the opposing African tectonic plate exposes the intact volcanic carapace that originally overlay much of the core complex. Mapping along an isochron across the center of complex showed that the central region, corresponding to the segment midpoint exposes largely granular plagioclase-free harzburgite, and virtually no dunite indicating little focused flow of melt through the mantle there [1]. In addition, while sampling the detachment fault surface itself recovered abundant pillow lavas and dike debris, remnants of the overlying hanging wall volcanic complex, little gabbro was found. This indicates that the volcanic complex was fed from magmatic centers to the north or south, and that locally the crust accreted at the midpoint of the segment consisted of dikes and volcanics intruded over the shallow mantle. To the south, however, dunite and wherlitic dunite (<5% Cpx), associated with granular harzburgite tectonites, are abundant. In the same area primitive troctolites, olivine gabbro and oxide gabbro intercalated with sheeted dikes are abundant, consistent with the delivery of primary MORB liquids at this point [2]. Further north, a second magmatic complex is exposed along the wall of the transform, while seismic reflection suggest yet another magmatic complex is situated directly east of the segment midpoint beneath the detachment fault surface. Thus, there is strong evidence for focused melt flow from the mantle at different points in time, suggesting that it is controlled by transient instabilities in the partially molten mantle beneath the ridge.

[1] Dick *et al.* G3, in press. [2] Lisenberg & Dick, in prep. [3] Canales *et al.,* in prep.

Mg isotopic composition of ferromanganese nodules from the Antarctic Circumpolar Current: A record of secular Mg isotope variation in seawater?

W.W. DICKINSON[1]*, M. SCHILLER[1], I. GRAHAM[2] AND J.A. BAKER[1]

[1]School of Geography, Environment and Earth Sciences, Victoria University, P.O. Box 600, Wellington, NZ (*correspondence: Warren.Dickinson@vuw.ac.nz)

[2]Geological and Nuclear Sciences, P.O. Box 30-368, Lower Hutt, NZ

Magnesium has a residence time of *ca.* 14 Ma in the oceans and is a major conservative constituent of seawater. A temporal record of the stable Mg isotopic of seawater during the Cenozoic would provide valuable constraints into the sources and sinks of Mg to the ocean. Such a record would also constrain the Mg/Ca Cenozoic evolution of seawater, which is critical to the use of this geochemical proxy in foraminifera when attempting to quantify changes in ocean temperatures.

Ferromanganese crusts and nodules preserve records of ocean chemistry over tens of millions of years, yet no stable Mg isotope data have been reported for the Fe-Mn oxyhydroxide phase of these authigenic sediments, which contains ca. 1 wt.% MgO. This reflects the difficulty in separating Mg from the chemically similar elements (Mn and Ni) that are present at high levels in ferromanganese materials by normal, nitric-acid-based, cation exchange methods.

We present the first analyses of stable Mg isotope variations in ferromanganese nodules, which were recovered from depths of ca. 4 km off the east coast of New Zealand and are bathed in the Antarctic Circumpolar Current. The nodules were dated by ^{10}Be methods and are up to 15 Myr in age. Mg isotope ratios were measured by MC-ICPMS after chemical purification of Mg from all other elements including Mn and Ni. Preliminary data suggest that secular variations in δ^{25}Mg over the past 8 Ma were minor with Mg stable isotopes being significantly lighter than modern seawater (ca. -0.7 to -0.8‰ with respect to DSM-3), but became significantly heavier (-0.2‰) between 8 and 10 Ma. Work is in progress to extend the record and its temporal resolution, along with an experimental study to investigate the sense and magnitude of Mg isotope fractionation associated with precipitation of Fe and Mg oxyhydroxides.

Hydrous sulphates formed during oxidation of colloform pyrite from Chiprovtsi Ag-Pb deposit, NW Bulgaria

D.A. DIMITROVA[1], V.G. MLADENOVA[2] AND L. HECHT[3]

[1]Geological Institute, Bulgarian Academy of Sciences, 1113 Sofia, Bulgaria (didi@geology.bas.bg)
[2]Sofia University "St. Kliment Ohridski", 1504 Sofia, Bulgaria (vassilka@gea.uni-sofia.bg)
[3]Natural History Museum, 10115 Berlin, Germany (lutz.hecht@museum.hu-berlin.de)

The Chiprovtsi Ag-Pb hydrothermal deposit, located in NW Bulgaria, comprises several metallic mineralizations, among which in the eastern part of the area occurs the low-temperature cinnabar-pyrite-fluorite mineralization. Pyrite is presented as grains, cubic and colloform habit. The latter one usually accompanies cinnabar formation followed by barite-calcite deposition. The colloform pyrite more easily reacts when exposed to air/aqueous oxidation because of its fine porous aggregate structure.

The studied samples also include metacinnabar, ankerite, fluorite and quartz. The colloform pyrite contains As up to 4.77 wt%, which is included during the oxidation-crystallization process in the newly formed sulphates, remaining in almost the same content (0.50-4.50 wt%). The oxidation process took place in room conditions (relatively low air humidity and 20-25°C). Mostly, the pyrite colloform aggregates during oxidation usually split along the elongation of the needle-like individuals (*c*-axis), which formed the spherulites. The pyrite sample disintegration to grainy powder is accomplished within 2-3 years.

The resulting efflorescent minerals were difficult to distinguish because of their complex occurrence and minute aggregate size. The following hydrous sulphates were identified using XRD and SEM-EDS with very good reliability: szomolnokite ($Fe^{2+}SO_4.H_2O$), aluminocopiapite ($Al_{2/3}Fe^{3+}_4(SO_4)_6O(OH)_2.20H_2O$), coquimbite ($Fe^{3+}_2(SO_4)_3.9H_2O$), halotrichite ($Fe^{2+}Al_2(SO_4)_4.22H_2O$) and voltaite ($K_2Fe^{2+}_5Fe^{3+}_3Al(SO_4)_{12}.18H_2O$). All of them occur as well formed micro- to nano-sized crystal habits: fibers (halotrichite), cubic and more complex combinative forms (voltaite), prismatic (szomolnokite), platy and platy-sheet hexagonal (aluminocopiapite and coquimbite, respectively), rounded (effect of partial dissolution).

The chemical reactions occurred release Fe^{2+} and H_2SO_4, followed by dissolution of the existing calcite and ankerite and further oxidation of Fe^{2+} to Fe^{3+}.

Silicon isotope variation of chert beds from later Archean to Proterozoic as a tracer of paleo-environmental variation in ocean

T. DING, D. WAN AND S. TIAN[1,2]

[1]Institute of Mineral Resources, CAGS, Beijing, China
[2]Key Laboratory of Isotope Geology, CAGS, Beijing, China

The silicon isotope compositions of chert beds from later Archean to Proterozoic have been investigated. The results are shown in Figure 1.

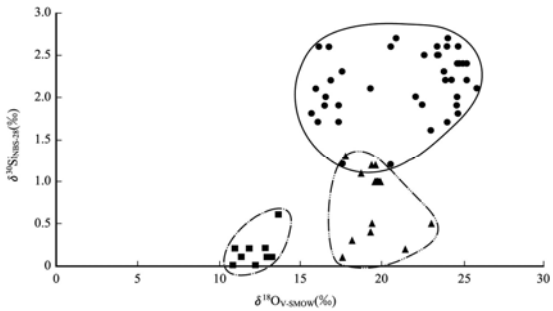

Figure 1: The relation between $\delta^{30}Si$ and $\delta^{18}O$ for some chert beds from later Archean to Proterozoic. ■ Later Archean Wutai Group; ▲Early Proterozoic Futuo Group; ● Middle Proterozoic Shisanling Group.

The $\delta^{30}Si$ values of quartz belts in banded quartz-sulfide formation of later Archean Wutai group vary from 0.0‰ to 0.6‰., with an average of 0.19‰. The $\delta^{30}Si$ values of chert belts in carbonate formation of early Proterozoic Futuo Group vary from 0.1‰ to 1.3‰, with an average of 0.76‰. The $\delta^{30}Si$ values of chert belts in carbonate formation of middle Proterozoic Shisanling Group vary from 1.2‰ to 2.6‰, with an average of 2.04‰. We know that the $\delta^{30}Si$ values of quartz in BIF formation of later Archean vary from -0.8 to -2.2, with an average of -1.28‰ [1]. There is a trend of increase of $\delta^{30}Si$ value from cherts of later Archean to early and middle Proterozoic, which is in consistent with the changes of paleo-environmental conditions in ocean, such as decrease of temperature and silicon content and increase of biological activity from Archean to Proterozoic.

[1] Ding *et al*. (1996) *Silicon Isotope Geochemistry*, Geological Publishing House, Beijing, China.

Adsorption behavior of Cu^{2+} on the surface of *Paenibacillus polymyxa*

Y. DING, X. LU AND Y. ZHOU

State key lab for mineral deposit research, Department of Earth Sciences, Nanjing University, China, 210093

The microorganism can clearly affect the mobility of the metal ions in the environmental fluids because of the abundant chemical groups on the cell surfaces. Adsorption of ions on the microorganism surface generally plays important roles in various biogeochemical processes, such as mineralization, nucleation and crystal growth. In order to disclose the adsorption mechanism and obtain the adsorption capacity of bacteria, we experimentally studied the Cu^{2+} adsorption behaviors of a widely occurring bacterium, *Paenibacillus polymyxa*.

Firstly, a series of consecutive acid titration was carried out. The results show that the range of the optimum pH value favoring the adsorption of proton on the surface of *Paenibacillus polymyxa*, is 7.54 to 6.00. It is also recealed that the cell surface bears abundant negative charges, which potentially determines the ion adsorption capacity. Secondly, the Cu^{2+} adsorption isotherm of *Paenibacillus polymyxa* was experimentally obtained. The Cu^{2+} adsorption amount is acquired based on the difference in the solution concentration before and after the adsorption experiment, which was measured using ICP-AES. The fitting analysis of the isotherm data indicates that the biosorption process agrees well with both Langmuir model and Freundlich model in the range of equilibrium concentration [Cu^{2+}] of environmental solution from 20×10^{-6}~1300×10^{-6}. According to the isotherm equation of Langmuir model, the calculated adsorption capacity of Cu^{2+} on cell surface is as high as 1.69×10^{-7} mg Cu/cell. Similar adsorption behaviors were also observed for the system involved strain *Steptomyces coelicolor* A3(2) and Cu^{2+}, Ni^{2+} [1], *Aeromonas caviae* and Cd^{2+} [2]. Furthermore, the pH of the solution increases linearly with the Cu adsorption amount increasing. It is deduced that ion exchange between surface H^+ and Cu^{2+} may be the potential mechanism of the apparent adsorption.

This study is supported by the Major State Basic Research Development Program of China (Grant No.2007CB815603) and Ph.D. Programs Foundation of Ministry of Education of China (Grant No. 20050284043).

[1] Doshi H, Ray A, & Kothari I L. (2007) *Current Microbiology*, **54** (3), 213-218. [2] Ozturk A, Artan T & Ayar A. 2004. *Colloids and Surfaces B-Biointerfaces* **34** (2), 105-111.

^{81}Kr dating and ^{85}Kr dating

Y. DING[1,2], Z.-T. LU[1,2,3], K. BAILEY[1], A.M. DAVIS[2,4], R.W. DUNFORD[5], S.-M. HU[6], W. JIANG[6], P. MUELLER[1], T.P.O'CONNOR[1], R. PURTSCHERT[7], N.C. STURCHIO[8], R. YOKOCHI[8] AND L. YOUNG[5]

[1]Physics Division, Argonne National Laboratory
[2]Enrico Fermi Institute, The University of Chicago
[3]Department of Physics, The University of Chicago
[4]Dept. of Geophysical Sciences, The University of Chicago
[5]Chemical Sciences and Engineering Division, Argonne National Laboratory
[6]Hefei National Laboratory for Physical Sciences at the Microscale, Univ of Science & Technology of China
[7]Institute of Physics, University of Bern
[8]Dept. of Earth & Environmental Sciences, University of Illinois at Chicago

Atom Trap Trace Analysis (ATTA) has been used to analyze two rare isotopes: ^{81}Kr ($t_{1/2}$=229,000 yr, isotopic abundance ~10^{-12}) and ^{85}Kr ($t_{1/2}$=10.8 yr, ~10^{-11}), in environmental samples. ^{81}Kr dating can now be used to determine the ages of groundwater samples in the range of 50,000–1,000,000 years. The present apparatus (ATTA-2) has an overall counting efficiency of 0.01% and, for ^{81}Kr dating, requires a water sample of 1,000 liters. We are developing a new apparatus (ATTA-3) to laser-trap and count ^{81}Kr atoms with the goal of reaching a counting efficiency of 1%, which would reduce the required sample size down to 10 liters of water or ice. If successful, ATTA-3 will enable a wide range of applications in the earth sciences.

This work is supported by NSF, Division of Earth Sciences, under Award No. EAR-0651161, and by DOE, Office of Nuclear Physics, under Contract No. DE-AC02-06CH11357.

(URL: http://www.phy.anl.gov/mep/atta/)

The onset of calcium carbonate nucleation: A computational study

D. DI TOMMASO* AND N. DE LEEUW

Department of Chemistry, University College of London, 20 Gordon Street, London WC1H 0AJ (*correspondence: uccaddi@ucl.ac.uk, n.h.deleeuw@ucl.ac.uk)

The formation of calcium carbonate ($CaCO_3$) from supersaturated solutions has been studied for more than a century as it represents a process of considerable importance, especially in the fields of CO_2 sequestration and biomineralization. It is now understood that the first step in the mineralisation of $CaCO_3$ is the homogeneous nucleation of amorphous particles [1], but the details of the onset of nucleation of the particles are still unclear. Our aim is to use a range of complementary computational methods to investigate the firts stages of the calcium carbonate nucleation process.

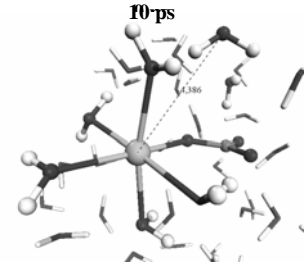

Figure 1: Representative snapshots from the CPMD.

Extensive Car-Parrinello molecular dynamics (CPMD) simulations of Ca^{2+}/CO_3^{2-} and Ca^{2+}/HCO_3^- immersed in water show that the formation of the monomer of $CaCO_3$ occurs through an associative mechanism (see Figure 1) and that the dominant building block of calcium (bi-)carbonate in aqueous solution is $Ca[\eta^1\text{-}(H)CO_3](H_2O)_5$, i.e. the preferred hydration number is five and the (bi-)carbonate is coordinated to the calcium in a monodentate mode [2]. This result agrees with static *ab initio* calculations, where a hybrid approach using a combination of explicit solvent molecules and a polarizable continuum model to treat the bulk of the aqueous environment has been applied to compute the solvation free energies of calcium bicarbonate species [2]. Based on this information, we consider the condensation reaction of calcium (bi-)carbonate particles in aqueous solution.

[1] D. Pontoni *et al*. (2003) *J. Phys. Chem. B* **107**, 5123-5125. [2] D. Di Tommaso and N. H. de Leeuw (submitted) *J. Phys. Chem B*.

Formation of membrane vesicles on cyanobacteria surfaces

M. DITTRICH[1], C. FISCHER[2], R. S. ARVIDSON[2] AND A. LUTTGE[2]

[1]EAWAG/ETH, CH-6047, Kastanienbaum, Switzerland (dittrich@eawag.ch)

[2]Department of Earth Sciences, Rice University, Houston, USA

Membrane Vesicles of Gram-negative Bacteria

Recent research has shown that membrane vesicles (MVs) are a common particular feature of the matrix of gram-negative bacterial biofilms [1]. The ubiquitous distribution of MVs is evident from observations of biofilms from a variety of natural and artificial environments. Experiments with planktonic biofilms demonstrate that MVs bind antibiotics and increase the sorption capacity of biofilms [1]. Because MVs mimic the bacterial cell surface, they should have strong, adhesive properties, possibly with specific adhesions for attachment. It has also been shown that environmental conditions may play a role in the expression of outer membrane of *Helicobacter pyroli* [2]. However, in spite of the tremendous effort to understand the contribution of MV to biofilms properties, our knowledge of the factors responsible for their formations is still limited.

Impact of Calcium on the MVs Formations

We have performed experiments with three different strains of cyanobacteria, i.e., *Synechococcus*-type: *Synechoccocus elongates*, *Synechococcus* Green, containing phycocyanin, and *Synechococcus* Red, containing phycoerythrin. The strains were washed two times and then exposed to CaCl2 solutions with different concentrations (0.6 mM, 1.5 mM, and 4mM) for periods ranging from 2 hours to 2 days. One set of samples were kept in the dark and the other was incubated under day-/night-light conditions. The surface properties of cyanobacteria strains were examined with vertical scanning interferometry (VSI [3]), an imaging technique that resolves sample surface features as small as 20 nm. Our results show that calcium ions impact the formation of MVs by *Synechoccocus* Green cells under day/night-light conditions at calcium concentrations between 0.6 and 4 mM. In the case of *Synechoccocus* elongates, MVs formed at [Ca] > 1.5 mM. By comparison, cell surfaces of *Synechococcus* Red were not strongly impacted by dissolved calcium. Our results suggest that MV formation is strain-specific and triggered by environmental calcium concentrations.

[1] Schooling & Beveridge (2006) *J. Bacteriol.* **188**, 5945-5957. [2] Keenan & Allardyce (2000) *J. Gastroenterol. Hepatol.* **12**, 1267-1273. [3] Davis & Luttge (2005) *Am. J. Sci.* **305**, 727–751.

Volatiles and trace elements in rejuvenated-stage lavas from Niihau, Hawaii: Evidence for carbonatite metasomatism

J.E. DIXON[1], D. CLAGUE[2], B. COUSENS[3] AND M.L. MONSALVE[1]

[1]University of Miami (j.dixon@miami.edu)
[2]MBARI (clague@mbari.org)
[3]Carleton University (bcousens@earthsci.carleton.ca)

We present volatile, trace element, and radiogenic isotopic compositions for Niihau rejuv-enated-stage lavas (RSL). These lavas display trace element heterogeneity greater than RSL from other islands, with enrichments in Ba, Sr, and LREE. Niihau RSL also have high and variable H_2O/Ce and Cl/La (620 and 39, respectively). We model trace elements of most RSL by small degrees (1-15%) of melting of depleted peridotite recently metasomatized by a few percent of an incipient melt from the Hawaiian plume. Compositions of Niihau RSL are best explained by addition of 0.1 to 0.4% carbonatite, to a depleted peridotite less enriched in incipient melt than the source of other RSL. Our model is consistent with deep melting of carbonated eclogite within the plume to produce carbonatite melt and silica-undersaturated silicate melts that metasomatize the surrounding mantle. The metasomatic component is best preserved at the margins of the plume sampled during flexural uplift-related melting.

Saprolite and the evolution of upland landscapes – Links between erosion and weathering in Sierra Nevada, CA

J.L. DIXON[1]*, A.M. HEIMSATH[2] AND R. AMUNDSON[3]

[1]Dartmouth College, Hanover, NH 03755 (*correspondence: jean.dixon@dartmouth.edu)
[2]Arizona State University, Tempe, AZ 85287
[3]University of California, Berkeley, Berkeley, CA 94720

Saprolite weathering is widely studied from a geochemical perspective; little attention, however, is directed to understanding what geomorphic role the saprolite system may play in influencing the patterns and rates of landscape evolution. We present an adapted set of equations to calculate rates weathering and physical erosion based on immobile elements and *in situ* produced cosmogenic ^{10}Be concentrations. Our approach differs from previous calculations of Riebe *et al.* [1] because we make the critical assumption that ^{10}Be derived rates of denudation reflect only soil production and cannot be used to derive total denudation rates in landscapes with deep saprolite (>2m) due to nuclide attenuation. Lastly, we present field data from a climate sequence in the western Sierra Nevada, CA that show previously unquantified links between weathering and soil mobility. Our field data show that the rate of physical erosion (21-88 $tkm^{-2}y^{-1}$) increases with saprolite weathering intensity and rate (20-137 $tkm^{-2}y^{-1}$). Fractional mass loss due to weathering ranges from 37-65% (as shown by the measurements of the immobile element Zr). Furthermore, soil and saprolite weathering are inversely related, whereby saprolites that experience the most weathering lie under weakly weathered soils.

We suggest that saprolite weathering reduces coherence of rock and increases transportability, thus reducing soil weathering by shortening residence times. Additionally, the nature of the relationship between physical erosion and saprolite weathering in the Sierra Nevada is modulated by dominant processes of sediment transport; sites eroding primarily by bioturbation display a stronger erosion-weathering relationship than our sites with abundant tree throw. This study quantifies feedbacks between saprolite weathering and physical and chemical processes in the soil and suggests that the saprolite system plays a very large and often overlooked role in the long term evolution of upland landscapes.

[1] Riebe *et al.* (2003) *GCA* **67**, 4411-4427.

Fluids role in formation of microdiamonds from ultrahigh pressure metamorphic terranes

L. DOBRZHINETSKAYA[1]* AND R. WIRTH[2]

[1]Department of Earth Sciences, University California, Riverside CA 92521, USA (*correspondence: larissa@ucr.edu)
[2]GeoForschungsZentrum, D-14473, Potsdam, Germany

Methods and Results

Metamorphic microdiamonds are known within six orogenic belts related to Paleozoic continent-continent collisons [1]. Our studies with a synchrotron infra-red (IR) spectroscopy and a transmission electron microscopy show that the diamonds contain nanometric fluid and crystalline inclusions of varing compositions incliding K, P, S, Cl, Si, Al, Ca, Mg, Fe and O. In the Kokchetav massif, the diversity of Si-, Al- and Fe- oxide nanoinclusions in diamonds correlates with the bulk chemistry of their host rocks (quartz-feldspathic gneisses, quartzite), whereas Ca- and Ca-Mg- carbonate inclusions mostly occur in diamonds from marbles. The fluid inclusions of the Erzgebirge diamonds contain Mg and Ca, but more often Si, Al and Ti. Other elements such as K, P, S and Cl occur in all fluid inclusions we have observed in any metamorphic diamonds regardless of their locations. Presence of OH-stretching bonds of molecular H_2O and CO_3^{2-} radicals were confirmed by synchrotron IR spectroscopy in both Kokchetav and Erzgebirge diamonds. Most diamonds are skeletal; if they are cubes or octahedra, a resorpsion is observed on their faces. The resorption is due to aqueous fluid ineraction with the diamond faces; this retrograded fluid triggers diamond transformation to graphite.

Discussion

Diamond-forming medium was suggested to be an ultrapotassic melt [2], or carbon-rich silicate melt [3]. Our results indicate that the diamonds originate from a supercritical COH fluid of crustal origin. The enrichment of such a fluid with K, P, S and Cl has no direct connection to any ultra-potassic intrusions, or Si-melts, but it reflects high solubility of these elements in a COH fluid at high pressures. Later aqueous fluid promotes diamond-to-graphite reactions or/and cuases the resoprion of diamond crystals surface.

[1] Dobrzhinetskaya *et al.* (2007) *Proc. Natl. Acad. Sci. U. S. A*. **104**, 9128-9132. [2] Hwang *et al*. (2006) *EPSL* **243**, 94-106. [3] Massonne (2003) *EPSL* **216**, 347-364.

Boron and Nitrogen in ultrahigh-pressure terrestrial rocks

L. DOBRZHINETSKAYA[1]*, R. WIRTH[2], J. YANG[3], H. GREEN[1], P. WEBER[4] AND I. HUTCHEON[4]

[1]Department of Earth Sciences, University of California, Riverside CA 92521, USA (*correspondence: larissa@ucr.edu)
[2]GeoForschungsZentrum, D-14473, Potsdam, Germany
[3]Key Laboratory for Continental Dynamics, Institute of Geology, Beijing, China, 100037
[4]Glenn T. Seaborg Institute, Lawrence Livermore National Laboratory, Livermore, CA 94551, USA

Methods and Results

Nitrogen is a well know constituent of diamonds from both kimberlitic sources and ultrahigh-pressure metamorphic terranes related to continent-continent collisions. It was also described in ilmenite xenocrysts from African kimberlites. We have recently discovered nanometric inclusuions of Boron Nitride and TiN – osbornite – in coesite associated with kyanite, FeTi alloy and OsIr alloy containing microdiamond inclusion; all are from massive chromitite of the mantle section of the Tibetan ophiolite. Both TiN and BN form bright-contrast particles in secondary-electron SEM images. Because EDS spectra of boron and nitrogen have severe overlaps with Ti L-lines, we have used EELS to confirm the presence of boron and nitrogen K-edges and to separate them from Ti L-lines. Electron diffraction data (TEM) identify the cubic boron nitride (c-BN) structure. TiN is stoichiometric (Ti=77.20wt%; N=22.80wt%) and has cubic symmetry, NaCl structure. NanoSIMS studies of osbornite show that its $\delta^{15}N$ = -10.4 ± 3 ‰, what is a characteristic of mantle nitrogen known in many kimberlitic diamonds.

Discussion

Because both nitrides are inclusions in coesite, high-PT conditions are required for their formation. We offer two hypotheses to explain their origin—astrobleme versus a mantle convection model. Astrobleme hypothesis is less favorable because there is not any evidence of impact microstructures in the host coesite and in the surrounding phases. We hypothesize that a small fragment of boron-rich Si-Al metasediments was subducted to mantle depth and due to mantle convection was brought to the midle-oceanic ridge ito be trapped by chromitite at the bottom of lower horizons of the Tibetan ophiolite formation. This is unexpected occurrence for B-bearing metasediments.

Mineralogical and geochemical studies of the Afyon volcanics, West Central Anatolia,Turkey: Preliminary results

G.D. DOĞAN[1]*, A. TEMEL[1] A. GOURGAUD[2] AND H. DEMIRBAĞ[3]

[1]Hacettepe University, Department of Geological Engineering, 06800, Beytepe-Ankara, Turkey (*correspondence: gdeniz@hacettepe.edu.tr) (atemel@hacettepe.edu.tr)

[2]Université Blaise Pascal, OPGC, Laboratoire CNRS "Magmas et Volcans" 5 rue Kessler-63038, Clermont-Ferrand Cedex, France (gourgaud@opgc.univbpclermont.fr)

[3]Maden Tetkik ve Arama Genel Müdürlüğü, Jeoloji Etüdleri Daire Başkanlığı G Blok, Ankara-Turkey (demirbag@mta.gov.tr)

This study represents mineralogical and geochemical characteristics of the Afyon volcanics which are located in the west central Anatolia, Afyon-Turkey. Samples were taken from lava flows, domes and, block and ash flows. Mineralogical and petrographical studies show that all the samples are fined-grained and exhibit porphyritic texture. Afyon volcanics consist of plagioclases, sanidine, phlogopite ($Mg\#_{74-94}$), biotite ($Mg\#_{53-66}$), amphibole, cliopyroxene, orthopyroxene, apatite, hematite and ilmenite phenocrysts. Microprobe studies reveal that plagioclases are identified as labradorite-oligoclase (An_{3-63}), amphibole minerals are tschermakite, richterite, magnesiohornblend ($Mg\#_{54-81}$), cliopyroxenes are diopside, augite (Wo_{43-47}) and orthopyroxenes are hypersthene (En_{40-74}) in composition. The presence of both normally and reversed zoned feldspars suggest that these volcanics can be affected by magma mixing process. Based on geochemical analyses Afyon volcanics are composed of trachyandesite, trachydasite and trachyte and, they have alkaline characteristics. Fractional crystallization process is observed from major element versus SiO_2 diagrams.

Aqueous geochemistry of Rhenium in sulfidic environments

M.K. DOLOR* AND G.R. HELZ

Chemistry and Biochemistry, University of Maryland, College Park MD 20742 (mdolor@umd.edu)

We explore the hypothesis that reaction with sulfide transforms Re from a highly soluble to a particle reactive form in reducing marine environments. Exposing perrhenate (ReO_4^-) to sulfide leads to formation of thioperrhenates ($ReO_nS_{4-n}^-$), which can be recognized by their characteristic UV-Vis absorption spectra. However, ReO_3S^- and ReS_4^- are the only thioperrhenates observed in experiments that have continued in some cases for more than 4 years. The intermediate thioperrhenates ($ReO_2S_2^-$ and $ReOS_3^-$) are apparently extremely unstable and short-lived, a result that was anticipated by Tossell [1] based on theoretical calculations. Sulfidation of ReO_4^- appears to be acid catalyzed, like the analogous sulfidation of MoO_4^{2-} [2].

Obtaining a stability constant for ReS_4^- is difficult because polymerization reactions intervene, interfering with optical determinations of ReS_4^-. Rhenium sulfide sols are produced and can be stable for years. To a first approximation, an equilibrium between dissolved and colloidal Re polymer in sulfidic waters can be represented by:

$$ReS_4^- + H^+ \leftrightarrow \tfrac{1}{2}\, Re_2S_7(coll) + \tfrac{1}{2}\, H_2S$$

Curiously, this reaction suggests that very low-sulfide pore waters, such as would be found in suboxic sediments, would be more favorable for colloid formation than highly sulfidic pore waters. However, the above reaction incompletely describes colloid formation, which seems to be enhanced by presence of polysulfides. Polysulfides have been found to be a structural element of the colloids [3]. Currently we are investigating the possibility that sorption of colloids by mineral surfaces fixes Re in suboxic sediments.

[1] Tossell J. A. (2005) *Geochim. Cosmochim. Acta* **69**, 2497-2503. [2] Erickson B. E. and Helz, G. R. (2000) *Geochim. Cosmochim. Acta* **64** 1149-1158. [3] Schwarz D. E., Frenkel A. I., Nuzzo R. G., Rauchfuss T. B., and Vairavamurthy A. (2004) *Chemistry of Materials* **16** 151-158.

Quantum mechanical insights on controls of Fe isotope fractionation

S.D. DOMAGAL-GOLDMAN[1]* AND J.D. KUBICKI[1,2]

[1]Deptartment of Geosiences,
The Penn. State Univ., University Park, PA 16802
(*correspondence: sgoldman@geosc.psu.edu)
[2]Earth and Environmental Sciences Inst.,
The Penn. State Univ., University Park, PA 16802
(kubicki@geosc.psu.edu)

We will present Molecular Orbital/Density Functional Theory (MO/DFT) calculations for a number of aqueous Fe-containing complexes, and use the results of these calculations to gain insights about controls on Fe isotope fractionations in common natrual and laborartory settings. Specifically, we will compare predictions of fractionation factors to predictions of structural and electronic features for these molecules. These comparisons will be used to determine the degree to which covalent bonding, coordination number, molecular mass, Fe association constant, oxidation state, and ligand charge affect the equilibrium Fe isotope fractionation factor of a complex.

The results we will present indicate that the effects of different molecular properties on the fractionation factor can be viewed through the lens of molecular geometry. The average lengths of the bonds made with the Fe atom and the coordination around the Fe atom act as controls on the fractionation factor, through which other properties have their effect. Consider, for example, the redox state of the Fe atom, which exhibits the largest influence on the fractionation factor of a complex. The reason for this dominant influence is the sizeable changes to bond length (and, therefore, bond strength) that result from changes to the oxidation state of the Fe atom. A secondary impact that metallic charge has on the fractionation factor is through changes in the coordination about the Fe atom: Fe(III)-bearing complexes are more likely to exhibit 6-fold coordination about the Fe atom, wheras Fe(II)-bearing complexes are more likely to exhibit 4- or 5-fold coordination about the central Fe atom. Thus, both the primary and secondary ways in which oxidation state affect fractionation factor can be explained and analyzed through consideration of impacts on the geometry of the Fe-ligand complex. Other properties that have a significant influence on fractionation factors can be treated in a similar manner.

This work will expand the set of molecules for which fractionation factors have been predicted, and will place previous experimental work in better theoretical context. We hope to use the conclusions form this work to motivate future studies of isotopic fractionations of other transition metals.

Study on water supply of palaeo lakes during pan-lake period of late Pleistocene in Alxa area, China

Z.H. DONG[1,2]* AND J.S. CHEN[2]

[1]State Key Laboratory of Hydrology-Water Resources and Hydraulic Engineering, Hohai University , Nanjing, China (*correspondence: donghzh@hhu.edu.cn)
[2]Research Academy of Hohai University, Nanjing210098, China

During late Pleistocene there was also palaeolakes in Alxa area. Present Tengger desert, Badain Jaran desert and Gurinai grassland used to be vast lakes. Based on the palaeo-lake deposits and landforms, and the primary analytic results on the typical sections, it was presumed that a vast continual fresh water lake existed in the Northwest area of Tengger desert in the period between 39~23 ka BP [1]. The paleaolake formed the that period is called Megalake Tengger.

Some researchers figured out that the form of paleaolakes in Alxa area attribute to large precipitation caused by local warm and wet climate. However, there are some doubtful points in above deduction. According to the isotopic study and hydro chemistry tests such as ^{14}C, $^{87}Sr/^{86}Sr$, δD, $\delta^{18}O$, T and CFC in Badain Jaran desert and adjacent area, it is proved that groundwater in Alxa area is recharged by water from Tibetan Plateau through deep fault [2].

Since there are groundwater discharge from deep faults to Alxa area, it is possible that the palaeo-lake water was not only from local precipitation but also from deep faults water transportation. Large volume of precipitation in Tibetan Plateau discharges to Alxa area and vast palaeo lakes came into being during late Pleistocene through a huge fault. This huge fault exist at least 42 ka and still water conductive till now.

There is actual geological evidence for the assumption of huge fault. Geological survey shows a series of fault systems such as Altun fault, Xigaze -Langshan fault and Zaduo-Yabulai fault existing in the north and east of Tibetan Plateau. It is a scientific question deserving further study to investigate whether surface and groud water in Tibetan Plateau supply the palaeo lake in Alxa area.

[1] H.C. Zhang *et al.* (1997) *Journal of Lanzhou University (Natural Sciences)* **33(2),** 87-91. [2] J.S.Chen *et al.* (2004) *Nature* **432**, 459-460.

Development of web-based framework oriented heterogeneous geochemistry data integration

S. DONG, H. YIN AND Z. WANG

Deparment of Earth Science, Nanjing University, Nanjing, 210093, China (dsc@nju.edu.cn)

Heterogeneous geochemistry data, originated from different sources, standards, terminologies and data formats leads to great problems in data sharing and integration [1]. These problems can be divided into three categories [2]: syntactic, structural and semantic heterogeneity. In order to make geochemistry data easily accessible, sharing, interoperable and visualized through the Web, we have developed a prototype of Web-based 4 tier framework based on metadata schema and ontology.

The four layers, from the bottom up, are the storage, description, service and application layer, respectively. The bottom layer, storage layer stories data sets in different formats. The relational database in the bottom layer and the geochemistry metadata schema encoded in XML in the second layer are used to handle the syntactic and structural heterogeneity. The geochemistry ontology based on SWEET and encoded in OWL in the second layer are responsible for the problem of semantic heterogeneity. The third layer, service layer contains browsing, searching, analyzing and some other Web services. The top layer, the application layer is oriented to the end user for data visualization and also provides interfaces for other Web-based applications. This prototype is flexible and is capable of extensibility.

We have applied this prototype to construct China Southeast Geochemistry Database. This framework is our first attemp to make large scale geochemistry data sets sharing and integration.

This work is financially supported by Nanjing University Pre-Research Grant: “Developing Ontology Framework for heterogeneous Geoscience data sharing”.

[1] Raskin, R. (2006) Development of ontologies for earth system science. *Geological Society of America* **397** pp. 195-199 [2] Sheth, A. (1998) Changing focus on interoperability in information systems, From system, syntax, structure to semantics. In Goodchild, M.. Egenhofer, M.. Fegeas, R.. and Kottman, C., eds., *Interoperating Geographic Information Systems*. Kluwer. pp. 5–30.

High-resolution radiocarbon calibration from 30-50 ka based on stalagmite ^{14}C and ^{230}Th ages

J.A. DORALE[1]*, J.R. SOUTHON[2] AND R.L. EDWARDS[3]

[1]University of Iowa, Iowa City, IA 52242, USA (*correspondence: jeffrey-dorale@uiowa.edu)
[2]University of California, Irvine, CA 92697, USA (jsouthon@uci.edu)
[3]University of Minnesota, Minneapolis, MN 55455, USA (edwar001@umn.edu)

We present a high-resolution radiocarbon calibration curve from 30-50 ka that in broad form agrees nicely with the calibrations of Hughen *et al*. [1] and Fairbanks *et al*. [2], but refines and potentially improves certain segments of the record, especially from 39-50 ka and a disputable section circa 36-37 ka. Our stalagmite-based calibration is based on 66 ^{14}C determinations, with 54 of those from 39-50 ka.

Because some of the carbon in calcite stalagmites is derived from carbonate bedrock, this dead carbon fraction (DCF) must be accounted for in the radiocarbon age determination. While we cannot rule out the possibility that our stalagmite DCF has varied through time, by assuming that it has not, and by appying a consistent DCF age offset of 2,600 years uniformly to all data points we have achieved a very good fit to the existing calibration curves of Hughen *et al*. [1] and Fairbanks *et al*. [2].

Our stalagmite-based calibration appears to offer a rare suite of strengths in comparison to the other available data sets used for calibration in this time period: 1) direct ^{14}C and ^{230}Th age determinations on the materials used for calibration, 2) equivalent or superior analytical precision for both ^{14}C and ^{230}Th age determinations, 3) very high resolution, and 4) no indication whatsoever of any diagenetic alteration, and a solid basis for ruling out diagenesis (dense, non-porous calcite). We believe these characteristics account for the integrity of the data set, which is impressively consistent in trend over the entire 30-50 ka period, contains no outliers requiring alternate hypotheses about the data, and appears more informative on the issue of calibration compared to the exisiting data sets in the relatively poorly constrained window from 43-50 ka. Finally, we do not observe in our data the large variations in $\Delta^{14}C$ reported by Beck *et al*. [3] from 40-45 ka.

[1] Hughen *et al*. (2004b) *Radiocarbon* **46**, 1059-1086. [2] Fairbanks *et al*. (2005) *Quat. Sci. Rev* **24**, 1781-1796. [3] Beck *et al*. (2001) *Science* **292**, 2453-2458.

Vegetation over hydrologic control of sediment transport over the past 100,000 yr

A. DOSSETO[1], S.P. TURNER[1], P. HESSE[2], K. MAHER[3] AND K. FRYIRS[2]

[1]GEMOC National Key Centre, Department of Earth and Planetary Sciences, Macquarie University, Sydney, Australia (adosseto@els.mq.edu.au)
[2]Department of Physiscal Geography, Macquarie University, Sydney, Australia
[3]Department of Geological and Environmental Sciences, Stanford University, USA

Uranium isotopes can be used to determine the residence time of sediments in a catchment, i.e. how long they are stored in weathering profiles and transported through the catchment by rivers. We have measured uranium isotopes in sediments from palaeo-channels of the Murrumbidgee River (Murray-Darling Basin, southeastern Australia) to quantify variations in sediment residence times over the past 100,000 years.

Results indicate that sediments transported through the Murrumbidgee catchment during the Last Glacial Maximum (LGM) resided for 10's of thousands of years in the catchment. This contrasts with modern and 100ka-old channel sediments where the residence time reaches values as high as 400,000-500,000 years. Variations in sediment residence time in the Murrumbidgee basin do not strictly follow changes in bankfull discharge but instead are correlated with shifts in vegetation and atmospheric CO_2. In the absence of significant glacial erosion in this basin during LGM, this is at odds with what is expected from the links between climate and erosion (a decrease in CO_2 and temperature is expected to induce a decrease in weathering and erosion). Vegetation may be the link between climate and sediment transport: sparse vegetation in the upper catchment allows significant hillslope erosion during LGM but dense woodlands in the Holocene and during the last interglacial inhibit sediment delivery to the river from hillslopes and sediments are derived from the re-working of old (a few 100s ka) alluvial deposits. These observations would suggest that (i) changes in hydrology cannot explain alone changes in sediment transport and (ii) the impact of climate change on catchment erosion is operating indirectly, via changes in vegetation type and density.

Geochemical signatures are driven by seasonal flow regimes in the Chena River near Fairbanks, Alaska

T.A. DOUGLAS[1], J.D. BLUM[2], K. KELLER[2], L. GUO[3] AND Y. CAI[3]

[1]Cold Regions Research and Engineering Laboratory, Ft. Wainwright, Alaska (Thomas.A.Douglas@usace.army.mil)
[2]University of Michigan, Ann Arbor Michigan
[3]University of Southern Mississippi

Carbon emission from permafrost degradation is a potential positive feedback to climatic warming. In addition, as permafrost melts mineral surfaces that were previously frozen are exposed to weathering, possibly providing a geochemical signature for enhanced seasonal permafrost melting. The Chena River watershed in central Alaska contains warm (-2ºC) permafrost at risk for degradation. We collected water from the Chena near Fairbanks, Alaska biweekly for a year to measure watershed geochemistry in different seasonal flow regimes. We measured major elements, $\delta^{18}O$, $^{87}Sr/^{86}Sr$ and carbon and nitrogen organic and inorganic species. Major element concentrations were linearly correlated with discharge except during the highest flows. Spring runoff represented flushing of snow melt with the lowest yearly $\delta^{18}O$ values. During a summer rainy period waters became incrementally higher in $^{87}Sr/^{86}Sr$ and $\delta^{18}O$ values as old water was flushed from the system. Winter flows represent the deepest flow paths with the lowest $^{87}Sr/^{86}Sr$ values and yearly average $\delta^{18}O$ values, likely characterizing mineral weathering. Dissolved organic carbon was linearly related to discharge except during spring melt. Our results suggest watershed geochemistry changes markedly during the year and flows can be categorized into six flow regimes. Strong seasonal controls on water chemistry imply long term monitoring campaigns in northern watersheds should apply at least seasonal sampling. Geochemistry of seasonal flow events must be characterized before relationships between melting permafrost and river geochemistry can be assessed.

The oxidative breakdown of acid azo dyes by Mn oxide mine tailings

C.E. DOWDING AND K.L. JOHNSON

School of Engineering, Durham University, South Road, Durham, DH1 3LE, UK

Introduction

The decolorisation of textile effluent is a pertinent issue in waste water treatment. Many biotreatment technologies achieve the reductive cleavage of the azo bond, which generates a range of aromatic amines that are colourless but significantly more carcinogenic than the parent azo compound [1]. Advanced oxidative techniques have been successfully employed to remove colour from waste effluents, however, these techniques are often expensive, thus the development of an oxidative textile water treatment technique utilising Mn oxide mining waste is appealing.

Discussion and Conclusions

The manganese tailings were reacted with two acid dyes (acid orange 7 and acid yellow 36) under a range of chemical conditions typically found in textile effluent. Results obtained using UV-visible spectroscopy, liquid chromatography mass spectrometry, high pressure liquid chromatograph and attenuated total reflectrance Fourier transform infrared spectroscopy show that the Mn oxide tailings succesfully decolourise the two acid dyes via an oxidative process. The terminal products have been identified as quinone type compounds. Reaction mechanisms, kinetics and orders have been established using *ex situ* and *in situ* spectrocopic techniques.

[1] Gottlieb, A., C. Shaw, A. Smith, A. Wheatley & S. Forsythe (2003) *Journal of Biotechnology* **101**(1), 49-56.

Cross-arc element mobility and prograde subduction metamorphism at the Kurile convergent margin

B.M. DREYER[1,2]* AND J.D. MORRIS[1]

[1]Washington University, Saint Louis, MO 63130
[2]Now at Monterey Bay Aquarium Research Institute, Moss Landing, CA 95039 (*correspondence: dreyer@mbari.org)

Changes in the trace element and isotopic composition of cross-arc transects observed in many arcs globally in part reflect changes in the composition and/or volume of the slab component that ultimately reaches the depths of magma generation [1-4]. To address the origins of these cross-arc changes, we present a recently completed chemical characterization of the slab inputs (sediment and altered oceanic basalt from ODP Site 1179) that complements new and existing cross-arc data of the volcanic outputs from the wide, active Kurile convergent margin in the NW Pacific.

Particularly useful in cross-arc studies are elements that are mobile across the subduction zone interface such as B, Li, Pb, As, Sb, Cs, U, Rb and cosmogenic ^{10}Be ($t_{1/2}$~1.5Ma). Elevated ^{10}Be concentrations in all Kurile lavas analyzed to date requires the incorporation of subducted sediment [5]. Mass-balanced mixing relationships between the local mantle and various chemical extracts of the incoming crust demonstrate that the strong slab-fluid signature in Kurile volcanic front (VF) lavas and the waning signal in rear-arc (RA) lavas can be effectively modelled as a result of progressive updip loss of fluid-soluble elements during slab dehydration associated with prograde subduction metamorphism. The simplest interpretation that can explain multiple trace element and isotope (Sr-Nd-Pb-Hf-Be) systematics is that the cross-arc geochemical behaviour is linked to a transition in the mode of slab extraction with increasing depth-to-slab, from fluid to melt-like, coupled with previous updip depletion of fluid-soluble elements; partial melting of slab sediments beneath Kurile RA volcanoes have been previously inferred based on Hf-Nd systematics [6]. Results of integrated cross-arc studies have implications for the thermal and mineralogical structure of convergent margins as well as long-term element and mass flux.

[1] Ishikawa & Nakamura (1994) *Nature* **370**, 205-208. [2] Ryan *et al.* (1995) *Science* **270**, 625-627. [3] Woodhead *et al.* (1998) *J. Pet.* **39**, 1641-1668. [4] Kimura & Yoshida (2006) *J. Pet.* **47**, 2185-2232. [5] Tera *et al.* (1986) *GCA* **50**, 535-550. [6] Tollstrup, D.L. *et al.* AGU Fall Meeting, 2007.

Evolution of flowpaths in an alpine watershed of the Colorado Front Range, USA

J.M. DRISCOLL[1]*, T. MEIXNER[1], W. WILLIAMS[2] AND N. MOLOTCH[3]

[1]Dept. of Hydrology and Water Resources, Univ. of Arizona, Tucson, AZ 85721, USA (*correspondence: driscoll@hwr.arizona.edu)
[2]INSTAAR, Univ. of Colorado, Boulder, CO
[3]Dept. of Civil and Environmental Engineering, Univ. of California, Los Angeles, CA

High elevation ecosystems are sensitive to climate and atmospheric deposition change. The end member mixing approach has brought limited improvement in understanding how these systems might respond to changes in process level forcing [1] since chemical end members are assumed to not react and therefore spatially differentiated flowpaths cannot be determined with this approach. Mixing between end members leads to chemically distinct water compositions.

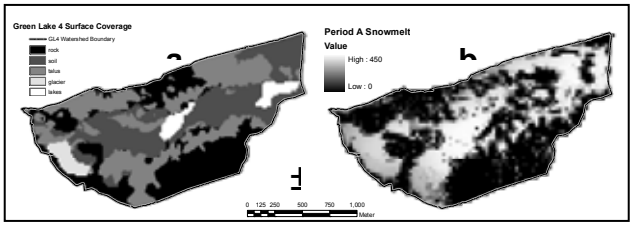

a) **b)**

Figure 1: a) End member distribution in the GL4 catchment, b) Snowmelt distribution in spring in the GL4 catchment.

Potential physical flowpaths in Green Lake 4 (GL4) watershed were determined using reactions between end members and the extent of mineral weathering using chemical data, the mineral assemblage and PHREEQC. Distribution of snowmelt over distinct periods was modelled to determine the contribution of each source water composition during the period. This coupled use of mixing models and the reaction path approach promises a better approach to understand catchment hydrology in reponse to changes in forcing.

[1] Liu, F. *et al.* (2004) *Water Resour. Res*. **40,** W09401.

Environmental voltammetry to characterize microbial habitats

G.K. DRUSCHEL[1], D. EMERSON[2] AND J.L. MACALADY[3]

[1]Dept. of Geology, University of Vermont, 180 Colchester Ave. Burlington, VT 05405 (gdrusche@uvm.edu)
[2]Bigelow Laboratory for Ocean Sciences, West Boothbay Harbor, ME 04575
[3]Department of Geosciences, Pennsylvania State University, University Park, PA 16802

Microbes in any natural environment utilize redox species as electron donors and acceptors to drive metabolic reactions, these redox species are often aligned in gradients that can vary in scale over many orders of magnitude. Voltammetric microelectrodes can be used to determine redox speciation *in situ*, in real time, and at spatial scales down to tens of microns. A number of microbially important redox species can be characterized with these electrodes, including a number of key sulfur and iron species, as well as oxygen, manganese, and other metals. We can couple this with tools to investigate microbial communities to describe geochemical niches that specific microbial communities inhabit, gather information about the microbial physiology of dominant organisms, and investigate the kinetics of microbial metabolisms under environmental conditions. We will present results from work with neutrophilic iron oxidizing microorganisms to describe kinetic controls on microbial habitat and from work on different communities of microbes associated with sulfuric acid speleogenesis in a cave system to illustrate the use of voltammetric microelectrodes to address these ideas.

Structure characters of continental red beds and their implications in the bottom of late Cretaceous Yaojia Formation in the Songliao Basin, NE China

X. B. DU*, X. N. XIE AND C. ZHANG

Faculty of Earth Resources, China University of Geosciences, Wuhan, 430074, China
(*correspondence: basindu@163.com)

High-resolution sequence stratigraphy, geochemistry and sedimentology studies were carried out on late Cretaceous Yaojia Formation in the Songliao Basin, northeast China indicated three types continental red beds occur at the bottom of the Yaojia Formation.

The type I is mainly characterized by pure and compact red mudstone formed in flooding plain or shallow lacustrine environments, there observed some Ostracoda fossils in the latter, which displaying features indicative of autochthonous deposits and oxidation during depositional process. The type II is featured by vermiculated red bed indicated gradually oxidation soil-forming process caused by groundwater gradual permeation during strata uplifting.The type III is composed of upper red mudstone and lower grey calcareous sandstone characterized by foaming encountered hydrochloric acid, which elucidates groundwater dissolving and schlepping calcium from mudstone permeates through red mudstone into lower grey sandstone after upper red mudstone stratum uplifts above groundwater table.

Because of gradually change of the underthrust angle of Pacific plate to Eurasian plate since 88Ma, the distinct regional characteristics of continental red beds are slowly thining from east to west in the Songliao Basin shows that eastern stratum uplifting is fiercer than in west. Meanwhile, seismic reflection images show that the bonudary surface between the Qingshankou and Yaojia formation is characterized by large scale truncation unconformity. We draw a conclusion that the continental red beds is a widespread second-order sequence boundary showed a long time exposure and oxidation process in early Yaojia Formation. The continental red beds are important for division of sequence stratigraphy and depositional system.

Evidence from Mo isotopic compositions for "A whiff of oxygen" before the Great Oxidation Event

Y. DUAN[1], G.L. ARNOLD[2], G.W. GORDON[1] AND A.D. ANBAR[1,3]

[1]School of Earth & Space Exploration, Arizona State University, Tempe, AZ 85287, USA (yun.duan@asu.edu)
[2]MPI for Marine Microbiology, Celsiusstr.1, D-28359, Bremen, Germany
[3]Dept. of Chemistry & Biochemistry, Arizona State University, Tempe, AZ 85287, USA

A high-resolution profile of Mo isotopic compositions has been obtained from a ~90 m continuous drill core recovered from the 2.5 Ga Mt McRae Shale in the Hamersley Basin, Western Australia, by the NASA Astrobiology Institute in 2004. 35 bulk samples reveal a large variation in δ^{98}Mo, ranging from 0.99‰ to 1.86‰. Relatively low and invariant δ^{98}Mo, clustering around 1.1‰, appears in the lower pyritic black shale unit (S2), followed by a gradual rise upcore. The largest δ^{98}Mo occurs within the upper pyritic black shale unit (S1) which also shows Mo enrichment relative to S2. In the rest of S1 and the overlying carbonate/marl unit, δ^{98}Mo declines while fluctuating heavily.

These sediments were likely deposited under locally euxinic conditions that facilitated quantitative Mo scavenging, and so the shift in δ^{98}Mo from S2 to S1 probably reflects change in the isotopic composition of Mo entering this basin. .

The previous finding of Mo and Re enrichments wthin S1 relative to S2 and the upper continental crust is interpreted as the evidence for a "whiff" of oxygen in the environment before the Great Oxidation Event [1]. The heaviest Mo isotope values are coincident with the metal excursion horizon and there is a mild correlation between bulk δ^{98}Mo and Mo concentration (r^2=0.56) through the core. Therefore, we hypothesize that increasing P_{O2} not only enhanced the rate of oxidative weathering, thus elevating the input of dissolved Mo to the ocean, but also led to increased formation of Mn oxides that trapped isotopically light Mo. This process generates isotopically heavy Mo in seawater today [2].

[1] Anbar *et al.* (2007) *Science* **317**, 1903-1906. [2] Arnold *et al.* (2004) *Science* **304**, 87-90.

From *ab initio* calculation to the prediction of thermodynamic properties of geological properties

Z. DUAN*, R. SUN AND Z. ZHANG

The Key laboratory of the Study of Earth's Deep Interior, Institute of Geology and Geophysics, Chinese Academy of Sciences, Beijing, 100029, China
(*correspondence: duanzhenhao@yahoo.com)

Using atomic site-site potentials to account for the angle-dependent molecular interactions with parameters directly from *ab initio* calculation results, We are able to predict the phase equilibria of CH_4 hydrate and CO_2 hydrate in binary systems over a wide temperature-pressure range (from 243–318 K, and from 10–3000 bar for CH_4 hydrate; from 253–293 K, and from 5–2000 bar for CO_2 hydrate) with accuracy close to experiment. This model is also capable of predicting the cage occupancy and hydration number for CH_4 hydrate and CO_2 hydrate without fitting any experimental data.

In another case of study, we use the *ab initio* potential surface across CO_2–H_2O molecules and carried out more than one thousand molecular dynamics simulations of the PVTx properties of the CO_2–H_2O mixtures in the temperature–pressure range from 673.15 to 2573.15 K up to 10.0 GPa. Comparison with extensive experimental PVTx data indicates that the simulated results generally agree with experimental data within 2% in density, equivalent to experimental uncertainty. The consistent and stable predictability of the simulation from low to high temperature–pressure and the fact that the molecular dynamics simulation resort to no experimental data but to ab initio molecular potential makes us convinced that the simulation results should be reliable up to at least 2573 K and 10 GPa with errors less than 2% in density. The success of these studies validates the predictability of *ab initio* intermolecular potentials for thermodynamic properties of geochemical systems.

Petrogenetic and metallogenic evolution of the West Cascades arc – A tale of thin crust

E.A. DU BRAY[1]*, D.A. JOHN[2] AND R.C. EVARTS[3]

[1]USGS-MS 973, Box 25046, DFC, Denver, CO, 80225 (*correspondence: edubray@usgs.gov)
[2]USGS-MS 901, 345 Middlefield Rd., Menlo Park, CA, 94025 (djohn@usgs.gov)
[3]USGS-MS 973, 345 Middlefield Rd., Menlo Park, CA, 94025 (revarts@usgs.gov)

Present-day High Cascades arc magmatism was preceded by ~40 m.y. of nearly co-spatial magmatism represented by the ancestral West Cascades arc. Time-space-composition relations for the West Cascades arc have been synthesized from a new compilation of >4000 geochemical analyses and associated age data. Neither the composition nor distribution of West Cascades magmatism was uniform along the length of ancestral arc through time. Initial (>40-35 Ma) West Cascades magmatism (mostly basalt-basaltic andesite) was focused at the north end of the arc between the present-day locations of Mt. Rainier and the Columbia River. From 35-17 Ma, initial basaltic andesite and andesite magmatism evolved to include dacite and rhyolite; magmatic activity became more voluminous and extended along most of the arc during this time. Between 17-7 Ma magmatism was focused along the arc segment coincident with the northern two thirds of Oregon and returned to more mafic compositions. Subsequent West Cascades magmatism was dominated by basaltic andesite to basalt compositions before the post-4-Ma onset of High Cascades magmatism. Transitional tholeiitic to calc-alkaline compositions dominated early (40 to ~25 Ma) West Cascades eruptive products, whereas younger rocks have a calc-alkaline affinity. Tholeiitic compositions characteristic of the oldest ancestral arc magmas suggest development above thin, immature crust, whereas the younger, calc-alkaline magmas suggest interaction with thicker, more evolved crust. The compositional transition is also reflected in the number and character of mineral deposits associated with the ancestral arc. Mineral deposits in West Cascades are uncommon and most are small relative to other continental arcs, probably reflecting thin, primitive crust that prevailed during most West Cascades magmatism. Low-grade porphyry copper deposits associated with rocks of the West Cascades arc in Washington, north of Mt. St. Helens, may be a consequence of Mesozoic continental crust beneath Washington but not farther south.

Sorption of iron from siderophore complexes by Mn oxides

O.W. DUCKWORTH[1]*, J.R. BARGAR[2] AND G. SPOSITIO[3]

[1]Department of Soil Science, North Carolina State University, Raleigh, NC 27695-7619, (*correspondence: owen_duckworth@ncsu.edu)
[2]Stanford Synchrotron Radiation Laboratory, 2575 Sand Hill Rd, Bldg 137, MS 69, Menlo Park, CA 94025 (bargar@slac.stanford.edu)
[3]Division of Ecosystem Science, University of California, Berkeley, CA 94720-3114 (gsposito@nature.berkeley.edu)

Siderophores are chelating agents produced by terrestrial and marine biota to increase the bioavailablity of ferric iron [1]. Recent work has suggested that both aqueous and solid-phase Mn(III) may affect siderophore-mediated iron transport [2, 3], but litte is known about the effects of manganese(III,IV) oxides. To probe the effects of layer type manganese oxides, which are a reactive component of soils and the oligotrophic marine water column [4], on the stability of aqueous Fe-siderophore complexes, the sorption of ferrioxamine B [Fe(III)HDFOB$^+$, an Fe(III) chelate of the trihydroxamate siderophore desferrioxamine B (DFOB)] to two synthetic birnessites [layer type Mn(III,IV) oxides] and a biogenic birnessite produced by *Pseudomonas putida* was examined. The Mn(III,IV) oxides greatly reduced the aqueous concentration of Fe(III)HDFOB$^+$ at pH 8. Fe K-edge EXAFS spectra suggest that the dominant fraction of Fe(III) associated with the Mn(IV) oxides is specifically adsorbed to the mineral structure at multiple sites, thus indicating that the Mn(IV) oxides displaced Fe(III) from the siderophore complex. These results indicate manganese oxides, including biominerals, may sequester iron from soluble ferric complexes, and thus we conclude that the sorption of iron-siderophore complexes may play a significant role in the bioavailability and biogeochemical cycling of iron in marine and terrestrial environments.

[1] Winkelmann, G. (1991) G. Winkelmann, Editor. CRC Press, Boca Raton. [2] Duckworth, O.W. and Sposito, G. (2005) *Environ. Sci. Technol*. **39,** 6037-6044. [3] Duckworth, O.W. and Sposito, G. E *Environ. Sci. Technol*. **39,** 6045-6051. [4] Tebo, B.M. *et al.* (2004) *Ann. Rev. Earth Planet. Sci.* **32,** 287-328.

High-pressure phases in the MgO-FeO-Al_2O_3-SiO_2 system: Implications for the deep mantle

T.S. DUFFY[1]*, A. KUBO[2], S. SHIEH[3], S. DORFMAN[1] AND V. PRAKAPENKA[2]

[1]Dept. of Geosciences, Princeton University, Princeton, NJ 08544, USA (*correspondence: duffy@princeton.edu)
[2]GSECARS, University of Chicago, Chicago, IL 60610, USA
[3]Dept. of Earth Sciences, U. Western Ontario, London, N6A 5B7 Canada

The discovery of the transition of $MgSiO_3$ from the perovskite (Pv) phase to the $CaIrO_3$-type (post-perovskite, pPv) structure is a key for understanding the Earth's deep mantle. FeO and Al_2O_3 are important components of the lower mantle and they can affect phase boundaries, equations of state, and other key properties. Using synchrotron x-ray diffraction techniques, we have examined perovskites and post-perovskites for selected compositions in the MgO-FeO-Al_2O_3-SiO_2 system over a wide pressure-temperature range.

For the MgO-Al_2O_3-SiO_2 system, powdered glasses with the bulk composition of X mol% $MgSiO_3$ and (1-X) mol% Al_2O_3 (X = 100, 95, 90, and 85) were used. *In situ* x-ray diffraction experiments at high pressures and temperatures were conducted at GSECARS, Advanced Photon Source. Our results demonstrate that Al_2O_3 incorporation into the pPv phase increases the transition pressure, transition width, unit cell volume, and decreases density, bulk modulus, and bulk sound velocity. The pPv phase transition in En95 composition, which is relevant to pyrolitic bulk composition, occurs at ~125 GPa at 2500 K, which corresponds to the condition at the top of D" layer. The pressure interval for the pPv phase transition in En95 bulk composition is ~7 GPa corresponding to a thickness of ~120 km, which is inconsistent with seismic observation of sharp D" discontinuity.

A series of experiments have also been carried out in the pyrope(Pyr)-almandine(Alm) system system for compositions corresponding to Alm38, Alm54, Alm73, and Alm100. We synthesized perovskites in all compositions at 70-90 GPa and ~2000 K, including Alm100 for the first time. We also show that Alm38, Alm54, and Alm73 transform to the post-perovskite phase above 140 GPa. Our results show that perovskites and post-perovskites with a wide range of Al_2O_3 and FeO compositions could exist under deep Earth conditions.

New production rate estimates for *in situ* cosmogenic ^{14}C

B. DUGAN, N. LIFTON AND A.J.T. JULL

Geosciences Department and Arizona Accelerator Mass Spectrometry Lab, University of Arizona, Tucson, AZ 85721 (bdugan@email.arizona.edu, lifton@email.arizona.edu, jull@email.arizona.edu)

Under the CRONUS-Earth project, a multidisciplinary investigation of terrestrial cosmogenic nuclide (TCN) production and measurement systematics, we aim to improve the calibration of *in situ* cosmogenic ^{14}C (*in situ* ^{14}C) production rates. *In situ* ^{14}C is unique among commonly measured TCNs by virtue of its short half-life (5.73 ka). Lifton *et al.* [1] estimated the *in situ* ^{14}C production rate in quartz based on measurements of wave-cut quartzite bedrock benches associated with the highstand of Pleistocene Lake Bonneville, Utah (17.4 ± 0.2 cal ka). To allow direct comparison of production rates for commonly measured TCNs in the same samples, CRONUS-Earth resampled the Lake Bonneville sites in 2005, and sampled Late-Glacial-age (11.6 cal ka) moraine and landslide deposits in northwest Scotland in 2006, as well as glacial deposits (15.5 cal ka) from the Puget Lowlands of Washington.

A more robust quartz pretreatment protocol than was employed by Lifton *et al.* [1] and Miller *et al.* [2], combined with improved extraction procedures, may necessitate a downward revision of the Lifton *et al.* [1] time-integrated site production rate estimate of up to 13.4%, from 52.9 ± 1.7 to 45.8 ± 2.1 ^{14}C at g^{-1} yr^{-1}. Initial data from new Lake Bonneville samples yield a time-integrated site production rate of 47.3 ± 0.8 ^{14}C at g^{-1} yr^{-1} - consistent with the revised estimate. Initial measurements of samples from 2 sites in Scotland have been completed as well. We are also investigating potential grain-size effects on measured *in situ* ^{14}C concentrations.

Modern production rate estimates for sea-level high latitude (SLHL) were calculated with each of 4 published production rate scaling models in order to compare results from the various sites. The Scotland samples consistently predict slightly higher modern SLHL production rates than those from Lake Bonneville (significant at 2σ). Weighted mean modern SLHL production rates from both sites range from 15.2 ± 0.3 at g-1 yr-1 for the Lal [3]/Stone [4] model to 17.5 ± 0.3 at g-1 yr-1 for the Lifton *et al.* [5] model. We will present additional measurements from all three sites to augment these initial results.

[1] Lifton et al. (2001) *GCA* **65**, 1953. [2] Miller *et al.* (2001) *Quat. Geochron.* **1**, 74. [3] Lal (1991) *EPSL* **104**, 424. [4] Stone (2000) *JGR* **105**, 23, 753. [5] Lifton *et al.* (2005) *EPSL* **239**, 140.

Pleistocene landscape evolution of a passive margin in response to climate change

T.J. DUNAI[1]*, B. EITEL[2] AND F.M. STUART[3]

[1]School of Geosciences, University of Edinburgh, EH8 9XP, Scotland, UK (*correspondence: tibor.dunai@ed.ac.uk)
[2]Geographisches Institut, Universität Heidelberg, D-69120 Heidelberg, Germany
[3]SUERC, East Kilbride, Glasgow G75 OQF, Scotland, UK

The Quaternary landscape evolution in Namibia, which is required to link offshore climate reconstructions to onshore processes, was heretofore largely unconstrained. Traditional terrestrial climate records are largely absent in the region. Landscape features in the region have the potential to record climatic signals, unaffected by episodic tectonic activity, since the post-beakup tectonic and large-scale landscape evolution in this region was largely concluded by the late Cretaceous [1].

We use exposure dating (^{10}Be, ^{21}Ne) of abandoned fluvial terraces and planation surfaces in the Ugab catchment, the second largest ephemeral river catchment in Namibia, to constrain periods of enhanced fluvial activity in southwestern Africa.

The data record episodes of significant Pliocene erosion. Regional pediments were abandoned at 1.1 Ma, 290 ka and 150 ka, and the level of the highest fluvial terraces was abandoned at 430 ka. The timings of these major fluvial episodes coincide with the largest Pleistocene shifts in the marine isotope record (glacial terminations II, III and V) [2] and the mode shift in orbital forcing from low-amplitude 41 kyr obliquity cycles to high amplitude 100 kyr eccentricity cycles.

In agreement with the interpretation of offshore records [3] we conclude that areas at the arid/semi-arid transition, such as in our study areas, are particularly sensitive transient climate. Rapidly increasing precipitation in barren catchments that had lost continuous vegetation cover in the preceding arid glacial periods is a likely mechanism for these transient erosion episodes in Namibia.

[1] Raab *et al.* (2005) *Tectonics* **24**, TC3006. [2] Lisiecki & Raymo (2005) *Paleooceanography* **20**, PA1003, doi, 10.1029/2004PA001071. [3] Dupont (2006) *Geochemistry Geophysics Geosystems* **7**, doi,101029/2005GC001208.

Integrated tephrochronology of the West Antarctic region - Implications for a potential tephra record in the West Antarctic Ice Sheet (WAIS) divide ice core

N.W. DUNBAR[1], W.C. MCINTOSH[1] AND A.V. KURBATOV[2]

[1]EES/NMBG, New Mexico Tech, Socorro NM, 87801
[2]Climate Change Institute 303 Bryand Global Sciences Center, Orono, ME, 04469

Of the many volcanoes that protrude through the West Antarctic ice sheet, Mt. Takahe and Mt. Berlin have been the most active ash-producers over the last 500,000 years. Mt. Takahe has produced a number of recent trachytic eruptions, including events at 8.2±5.4 ka, 93.3±7.8 ka and 102±7.4. Mt. Berlin has produced young events sampled in the crater region at 10.3±5.3, 18.2±5.8, 25.5±2.0. Further information about eruptions from Mt. Berlin is gained by studying a long section of exposed blue ice and intercalated tephra layers at Mt. Moulton. Eight of these tephra layers have been directly dated using $^{40}Ar/^{39}Ar$ geochronology of potassic feldspar phenocrysts, to 10.5±2.5; 24.7±1.5; 92.1±0.9; 104.9±0.6; 118.1±1.3; 135.6±0.9; 225.7±11.6; and 495.6±9.7 ka.

A total of 36 tephra-bearing layers have been recognized in the Siple Dome A ice core. The source volcanoes for these tephra layers are largely found within the Antarctic plate, although some South American and possibly a New Zealand volcano are also represented. Statistical geochemical correlations have been made between 12 of the tephra layers and source volcanic eruption. Ten of the tephra layers are correlated to known tephra layers found at Mt. Moulton or Mt. Berlin. One correlation is also made to the 8.2±5.4 ka eruption of Mt. Takahe. The existing ice core chronology agrees well with independently determined chronologies for the source eruptions.

The WAIS Divide ice core is located in central West Antarctica, in reasonably close proximity two the two main West Antarctic tephra-producing volcanoes, Mt. Takahe and Mt. Berlin, and is therefore likely to contain a number of known tephra layers from the two volcanoes. The youngest widespread tephra layer from a West Antarctic volcano is the 8.2 ka eruption from Mt. Takahe, and this layer is likely to be present in the WAIS Divide core. Mt. Berlin is likely to dominate the tephra record in the lower part of the core, and at least some of the tephra present at Mt. Waesche, Mt. Moulton and Siple Dome sites are likely to be found. Discovery of these layers in the WAIS Divide core could provide a number of useful cross-correlated time-stratigraphic markers linking the climate records.

Magma evolution in time and space at Volcán Llaima (38.7° S, Andean Southern Volcanic Zone - SVZ, Chile)

M.A. DUNGAN[1], C. BOUVET DE MAISONNEUVE[1], D. SELLES[2], J.A. NARANJO[3], S. ESCRIG[2] AND C. LANGMUIR[2]

[1]University of Geneva, Section of Earth Sciences, 13 rue des Maraîchers, 1205 Geneva, Switzerland (michael.dungan@terre.unige.ch)
[2]Harvard University, Earth and Planetary Sciences, Cambridge, MA 02138 USA (dselles@fas.harvard.edu)
[3]SERNAGEOMIN, A. Santa Maria 0104, Providencia Santiago, Chile (jnaranjo@sernageomin.cl)

Late Quaternary Volcán Llaima is a dominantly mafic to andesitic frontal-arc edifice (seven major eruptions and many smaller events since 1640). Holocene activity began ~13.5 ka by caldera collapse and eruption of the regional basaltic to andesitic (~52-58% SiO_2) Curacautin Ignimbrite. The Holocene edifice buried this caldera and was constructed mainly from a N-S central-vent system that is ~parallel to the adjacent Liquiñe-Ofqui Fault Zone. Mafic lavas and tephra (~51-55% SiO_2) have erupted with increasing frequency during the last ~3500 years. Magmas erupted from a partly circumferential system of flank fissures (oblique to the main cone's vent orientation) are typically more evolved and are derived from more diverse parental magma compositions. The most primitive erupted magmas are evolved basalts (<6.5% MgO) with relatively low incompatible element abundances compared to volcanoes behind the frontal arc and to those located north of 38° S. Phenocryst assemblages in mafic magmas are PL>OL>CPX>SP. Hydrous phases are absent from the most evolved pyroclastic unit (~69% SiO_2). Fractional crystallization apparently dominates differentiation from evolved basalt to andesite, although the vast majority of coarse mineral grains are out of equilibrium with host liquids: magma mixing appears to account for most of the open-system contributions. Parental magma diversity at Llaima is low and typical of this part of the southern SVZ (38-41° S), and it is far less than what is present at the Tatara-San Pedro complex (36° S). These new results are the foundation of an assault on the Llaima magmatic system designed to quantify mantle source-region parameters in the context of an understanding of how Llaima magmas ascend, interact, evolve and erupt.

Upper limits on the irradiation-induced short lived nuclei in comets

J. DUPRAT[1] AND V. TATISCHEFF[1,2]

[1]CSNSM-IN2P3-CNRS and Univ. Paris-Sud, F-91405 Orsay Campus, France
[2]CSIC-IEEC, Campus UAB, Fac. Ciencies, 08193 Bellaterra, Barcelona, Spain

The first results from the STARDUST mission [1] strengthen theoretical frameworks such as the *x-wind* model [2] in which high temperature minerals processed at a close distance to the nascent star have been transported to the comet forming region. Within the *x-wind* framework, several authors proposed that irradiation at close distance from the building star could account for the production of several short-lived radionuclei (SLR) that were once alive in the early solar system [3, 4]. We address here the issue of the total amount of nuclei that can be synthesized within such a process. Using global energetic constraints obtained from X-ray observations of young stellar objects and an updated nuclear reactions survey, we calculated upper limits on the amount of SLR that can be produced by nonthermal nucleosynthesis in the early solar system [5]. We show that ^{10}Be and ^{41}Ca can be produced by *in situ* irradiation of bare solids at levels reported in asteroidal material (meteorites) up to the comet forming region. ^{53}Mn and ^{36}Cl cannot be co-produced by irradiation together with ^{10}Be and ^{41}Ca at the canonical values currently reported (see Ref. [6] for a recent review). If future works confirm the high ^{7}Be/^{10}Be ratio inferred by [7] it may point toward the irradiation of a gas phase. Finally, we show that the maximum amount of irradiation-induced ^{26}Al can barely account for a maximum homogeneous rocky reservoir of 2-3 Earth mass (i.e equivalent to the inner solar system). Moreover, if CAIs did form in the embedded stellar stage, the well-defined canonical ^{26}Al/^{27}Al ratio observed in these objets is difficult to reconcile with an irradiation origin. The search for extinct ^{26}Al in STARDUST samples is of great importance since its discovery at a level similar to the one reported in meteorites would indicate a nucleosynthetic origin external to the solar system. This work was supported by ANR grant 05-JC05-51407 and by AGAUR grant 2006-PIV-10044.

[1] Brownlee *et al.* (2006) *Science* **314**, 1711-1716. [2] Shu *et al.* (1996) *Science* **271**, 1545-1552. [3] Lee *et al.* (1998) *APJ* **506**, 898-912. [4] Gounelle *et al.* (2001) *APJ* **548**, 1051-1070. [5] Duprat & Tatischeff (2007) *APJ*, L69-L72. [6] Wasserburg *et al.* (2006) *NPA*, **777**, 5-69 [7] Chaussidon *et al.* (2006) *GCA*, 224-245.

Experimental study of biomineralization processes relevant to CO_2 geological sequestration

S. DUPRAZ*, M. PARMENTIER, B. MENEZ AND F. GUYOT

IPGP, Centre de Recherches de Stockage Géologique du CO_2 (IPGP/TOTAL/SCHLUMBERGER) Paris, France (*correspondence:dupraz@ipgp.jussieu.fr)

Geological storage of CO_2 is an important option envisaged to mitigate enhanced CO_2 atmospheric greenhouse effect in the coming decades. It requires however the ability to model the behavior of carbon dioxide into deep geological reservoirs and to predict its fate for thousands of years following the injection. For this purpose, identification of the critical controlling processes and a proper understanding of their physics and chemistry are strongly required. The discovery of extensive and active microbial populations in deep environments had also lead to consider biologically mediated processes potentially critical to CO_2 sequestration itself. Of particular importance is the potential of microorganisms to promote mineral trapping of CO_2 through biomineralization. Little is known, however, about the biochemical processes involved and consequently, biocomponents are rarely taken into account in numerical modeling. In accordance, a joint experimental and numerical study was carried out to shed light on these interactions. Three different microorganisms, known as reference in biomineralization process (*Bacillus pasteurii*) or as endogenous species of potential storage sites (*Desulfovibrio longus* & *profondus*) were used for this purpose. Strains were exposed to various temperatures, salinities and gas compositions in an artificial minimal media representative of deep groundwaters from the basin of Paris (France), a potential location for CO_2 sequestration. A newly developed biomineralization control cell (BCC) allowed continuous measurement of pH, temperature, pressure, ORP, conductivity, $\{Ca^{++}\}$ and optical density at 600nm. Sequences of biomineralization (i.e. nucleation and growth) were established by means of SEM, TEM investigations together with X-ray absorption spectroscopy and Raman confocal imaging. First results demonstrate the important role of gas transfers in these processes as well as the specific influence of calcium ions on general metabolism. Overall, these developments bring new methodology to integrate experimental and computational approaches to finally better predict and interpret biogeochemical processes in the subsurface.

Experimentally major and trace partitioning between calcitic melt and calcite at 1000 bars

C. DURAND* AND L. BAUMGARTNER

Institut de Minéralogie et Géochimie, Université de Lausanne, l'Anthropole, 1015 Lausanne, Switzerland (*correspondence: Cyril.Durand@unil.ch)

The aim of this study is to understand the partitioning of major and trace elements between calcite and calcitic melts at near surface conditions (1000 bars) in the presence of water. Similar experiments have been already carried out by Wyllie and Tuttle [5]. Their study suggested a calcite melting temperature of 740°C. This calcite melting curve appears to be independent of the calcite/water ratio. The authors further suggest that hence, calcite melting could occur during contact metamorphism, as also suggested by studies on natural rocks [1, 2, 4]. Geochemical tracers could point towards the presence or absence of a carbonate melt in such an environment.

Our experiments were performed in rapid-quench cold-seal pressure vessels. Temperatures were varied in between 600 and 800°C. Gold capsules were charged with natural or artificial calcite. The letter was further enriched with different carbonates ($MgCO_3$, $FeCO_3$, $MnCO_3$, $BaCO_3$ and $SrCO_3$) as well as REE solution. Low calcite/water ratios were used to ensure enough melt for chemical analyses. Run durations vary in between 1.5 to 90h. Calcitic melts seem to be homogeneous without evidence for chemical zoning. Preliminary results show that Mn and Sr partition equally in between calcite and melt. All others chemical elements are preferentially enriched in the melt. The REE enrichment in the melt appears without fractionation between LREE and HREE. Hence, our initial experimental results indicate that the presence of melt can be unequivocally identified when it can be compared to the unmelted calcite, but it might be difficult to identify when the calcitic melt has migrated.

[1] P. Jutras *et al*. (2006) *Geol. J*. **41,** 23-48. [2] D.R. Lentz (1999) *Geology* **27,** 335-338. [3] I.V. Veksler *et al*. (2000) *Contrib. Miner. Petrol.* **138,** 27-34. [4] T. Wenzel *et al*. (2002) *J. Petrol.* **43,** 2049-2074. [5] P.J. Wyllie & O.F. Tuttle (1960) *J. Petrol.* **1,** 1-46.

The character and composition of fluid in equilibrium with peridotite in subduction zones

O. DVIR AND R. KESSEL

Institute of Earth Sciences, The Hebrew University of Jerusalem, Jerusalem Israel, 91904

Accurate determinations of the effect of water on the composition of liquid coexisting with peridotite are necessary to advance our understanting of the physical processes involved in melt generation at convergent plate margins. Experimental data bearing on hydrous peridotite dehydration and melting remain, however, sparse. We report experimental results of fluid and melt composition in equilibrium with peridotite measured using a novel freezing stage laser-ablation ICPMS following high pressure and temperature diamond-trap experiments on the rocking multi-anvil apparatus. We used this technique to directly characterize the fluid phase coexisting with synthetic (NCFMASH) peridotite at pressures of 4 and 6 GPa and temperatures between 700-800°C and determine the major element coomposition of all solid and fluid phases.

Our results indicate that at 4 and 5 GPa a fluid containing ~56 wt% H_2O coexists with peridotite up to 750°C while a hydrous melt containing 35 wt% H_2O is the stable phase at 800°C, indicating that the solidus lies between 750 and 800°C at this pressures. The solidus lies between 700 and 750°C at 5 GPa. These results indicate that the second critical endpoint is above 6 GPa.

Biofilm structure and biochemistry with soft X-ray scanning transmission microscopy

J.J. DYNES[1,2], T. REMA[3], A.P. HITCHCOCK[1], D.R. KORBER[3], G.G. LEPPARD[4], G.D.W. SWERHONE[2], M. OBST[1,5] AND J.R. LAWRENCE[2]*

[1]BIMR, McMaster University, Hamilton, Canada
[2]Environment Canada, Saskatoon SK, Canada (*correspondence: john.lawrence@ec.gc.ca)
[3]Food and Bioproduct Sciences, University of Saskatchewan, Saskatoon, SK, Canada
[4]Environment Canada, Burlington, ON, Canada
[5]Canadian Light Source, Saskatoon, SK, Canada

Biofilms are microbial communities consisting of single or multiple species (e.g., bacteria, algae, fungi) surrounded by an extracellular matrix, with complex architectures and biochemistry. The mapping of the distribution of macromolecules (e.g., protein, lipids, polysaccharides) and bioaccumulated antimicrobial agents in microbial biofilms is highly relevant to understanding biofilm formation, manipulation, and control. The analytical capability of soft X-ray scanning transmission X-ray microscopy (STXM) can be useful to probe how the nature, distribution, and role of macromolecules is affected by antimicrobials in antimicrobial-challenged biofilms.

Single species or mult-species natural biofilms were grown in flow-cells or rotating annular reactors, either in the presence or absence of antimicrobial agents. Quantitative component maps were derived for the macromolecules and of selected antimicrobials by spectral fitting of C 1s image sequences using linear regression procedures.

Discussion of Results

STXM provided evidence that the morphology of the cells, as well as the spatial distribution and relative amounts of the macromolecules in the biofilms and within the cells were different for each microbial species and antimicrobial. Cellular morphological and biochemical changes were indicative of adaptive responses and are specific to the antimicrobial agent applied and microbial species.

This presentation will show how STXM is improving our understanding of bacterial resistance mechanisms in antimicrobial-challenged biofilms.

We thank D. Kilcoyne, T. Tyliszczak (ALS); K. Kaznatcheev, C. Karunakaran, D. Bertwistle (CLS-SM). Study supported by NSERC, AFMNet, Canada Research Chair. ALS supported by DoE-BES. CLS supported by NSERC, CIHR, NRC and the University of Saskatchewan.

Origin of a carbonate-hosted gem corundum occurrence in southeastern British Columbia

T.J. DZIKOWSKI*, G. DIPPLE AND L.A. GROAT

University of British Columbia, Vancouver, BC V6T 1Z4 (*correspondence: tdzikowski@eos.ubc.ca)

Despite much previous research, the origin of gem corundum (Al_2O_3) deposits remains unclear, and as a result only primitive exploration strategies exist for different deposit types. The newly discovered marble-hosted Goat sapphire and ruby occurrence in British Columbia was studied to: (1) characterize the mineralization; (2) develop a genetic model for mineralization at this occurrence; and (3) develop an exploration strategy for gem corundum in carbonate-hosted deposits.

The corundum-bearing marble is hosted within pelitic and calcareous schist within the Paleozoic Monashee cover sequence near the Frenchman Cap dome. There are three types of laminations within the marble: (1) diopside-bearing laminations; (2) apatite ± K-feldspar ± zoisite ± pyrite ± titanite-bearing cataclastites; and (3) Cr-muscovite and phlogopite schist laminations which can host gem corundum. Peak metamorphic assemblages within the micaceous laminations are corundum + calcite + muscovite + rutile + anorthite + K-feldspar ± diopside. Lenses enriched in muscovite within the laminations are rimmed by K-feldspar and anorthite. Corundum is formed at or near peak metamorphic conditions on the high temperature side of the equilibrium: muscovite corundum + K-feldspar + H_2O.

Oxygen stable isotope data of coexisting calcite ($\delta^{18}O$=15.0 to 15.1 ‰ ± 0.1) and corundum ($\delta^{18}O$=10.9 to 11.1 ‰ ± 0.1) give $\Delta^{18}O_{cal\text{-}cor}$ = 4.0 to 4.2 ‰. These data are consistent with equilibrium fractionation at peak metamorphic conditions with temperatures between 500-600 °C.

A novel technique for species-specific Hg isotope ratio measurements using Hg-Thiourea complex ion chromatography

M. DZURKO[1]* AND H. HINTELMANN[2]

[1]Trent-Queen's Graduate Program, Trent University, Peterborough, On, Canada (*correspondence: mdzurko@trentu.ca)

[2]Chemistry Dept., Trent University, Peterborough, On, Canada (hhintelmann@trentu.ca)

Measurements of the natural fractionation of mercury (Hg) isotopes are a powerful tool to directly identify biogeochemical processes controlling the fate of mercury in the environment. In this study, we investigate the possibility for Hg isotopes to undergo biological fractionation during bioaccumulation in aquatic food webs.

The investigated technique permits the separation of monomethyl Hg (CH_3Hg^+) and mercuric Hg (Hg^{2+}) from water and biota on the basis of the difference in charge of their respective thiourea ($S=C(NH_2)_2^0$) complexes. A cartridge containing thiol-functionalized silica resin traps Hg^{2+} and CH_3Hg^+ from prepared sample solutions without retaining interfering sample matrix components and is capable of eluting the Hg species without the need for any further chromatographic separation.

An on-line Hg reduction technique using stannous chloride as the reductant is applied for accurate and precise mercury isotope ratio determinations by Cold Vapour - Multi-Collector Inductively Coupled Plasma - Mass Spectrometry (CV-MC-ICP/MS).

The results from this study may show that Hg isotope ratios could be used as a tracer technique to provide important information into the sources, and biogeochemical cycling of natural and anthropogenic Hg.

Changes to oil fluorescence by the invasion of gas or water

P. EADINGTON[1]*, R. KEMPTON[1], S. GEORGE[2], H. VOLK[1], J. BOURDET[1] AND C.E.S. COEHLO[3]

[1]CSIRO Petroleum Research, PO Box 1130, Bentley, WA, (*correspondence: Peter.Eadington@csiro.au)

[2] Department of Earth and Planetary Sciences, Macquarie University, Sydney, NSW 2109, Australia

[3]Petrobras Research & Development Centre, Av. Jequitiba, Ilha do Fundao, 21941-598 Rio de Janeiro, RJ, Brazil

Fluid inclusions that trap residual oil after most has drained from a reservoir have attributes that reflect interaction with imbibing (invading) gas or water.

Grains in oil reservoirs often contain one or more oil inclusions that collectively constitute oil inclusion assemblages (OIAs). Grains containing oil inclusions (GOI™) is the proportion of reservoir grains that contain one or more OIA. Fluorescence colour, location in the grain, and size of the gas bubble are three of eight attributes assigned to OIAs in GOI determinations samples from two wells on the North-west Shelf Australia.

At Jabiru 1A the predominant OIA in samples from the current oil zone has oil inclusions with uniform near-blue visual fluorescence. Only samples from the residual zone contain an OIA with near-white to near-blue fluorescence. At Gas Well A, which has an oil leg, there is an OIA that is comprised of near-yellow fluorescing inclusions with small gas bubble and inclusions with a large gas bubble that nearly fills the chamber and a rim of near-blue fluorescing oil.

In the field where water imbibed, the shift of fluorescence colour to near-white is consistent with lower mono-aromatic molecules having dissolved into the imbibing water. In the field where gas imbibed there is a shift to near-yellow fluorescence of oil inclusions consistent with enrichment of oil in heterocycles, and inclusions in the same OIA containing gas with a rim of near-blue fluorescing oil consistent with the imbibing gas having dissolved light hydrocarbons.